

# Motion of a Spinning Symmetric Top

V. Tanrıverdi

tanriverdivedat@googlemail.com

February 20, 2019

## Abstract

We first reviewed the symmetric top problem, then we have numerically obtained solutions of different possible motions. We have given an explanation about the rise of the symmetric top during nutation in terms of torque and angular momentum. We have encountered with previously unnoticed properties of motion and studied them. During the study, calculations gave some surprising results that the symmetric top can change its spin direction.

## 1 Introduction

Since child's top has very special properties, many people are interested in its motion starting from antiquity and the symmetric top problem became one of the long-studied topics of physics. The study on this topic starts with Euler and continues through Lagrange, Kovalevskaya and so on. Its unintuitive motion, nutation and precession are some of the interesting properties of the symmetric top.

The unintuitive property of the symmetric top is related to its being a non-inertial system. In our daily life, in general, we are familiar with inertial objects and this makes non-inertial object's motion unintuitive. Euler has obtained equations describing such motions of rotating rigid bodies under the influence of torque, these are known as Euler equations.

These equations can result in some complicated coupled equations and sometimes obtaining their solution analytically is impossible. This problem is studied with geometric techniques related to our historical background.

One of the important works with these geometric techniques on this problem is given by Routh in his book[1], which has explanations on sleeping top and eight different types of motion. There is also another work involving geometric techniques written by Klein and Sommerfeld[2]. They discuss different types of motion and regular precession.

There are more books involving chapters on the symmetric top problem, and some of them use a technique based on conservation of energy and angular momenta[3, 4, 5], usage of these is related to previous works on the problem with geometrical techniques. This technique is a bit hard to imagine since mathematical transformations and functions hide physical motion. Some other books on classical mechanics and dynamics or symmetric top include the effective potential, and they are a bit easier to imagine[6, 7, 8, 9, 10]. Some of these books also include the technique based on conservation of energy and angular momenta.

In this work, we will deal with the problem in a detailed way by using the effective potential and we will give physical explanations. In section [2], we will firstly review the symmetric top problem and obtain equations by using Euler equations, and then we will shortly review the problem in terms of Lagrangian and energy. In section [3], we will study the symmetric top problem with examples by using the effective potential and conservation of energy and angular momentum, we will also give explanations in terms of torque and angular momentum. We will study on sleeping top, regular precessions and ten different types of motion. In section [4], we will give a summary of some important points.

## 2 Symmetric top

### 2.1 Euler angles and Angular velocities

We can define rotations of rigid bodies with Euler angles. Let us consider two reference frames; one is stationary  $S'(x', y', z')$  and the other one is fixed to the rotating rigid body  $S(x, y, z)$ .  $\phi$  defines the rotation of the rigid body around stationary  $z'$ -axis;  $\theta$  defines the rotation of the rigid body around the lines of nodes, which is obtained by the intersection of stationary  $x'y'$ -plane with body  $xy$ -plane;  $\psi$  defines the rotation around body  $z$ -axis. These three angles, the line of nodes, the stationary and body reference frames are shown in Fig. 1.

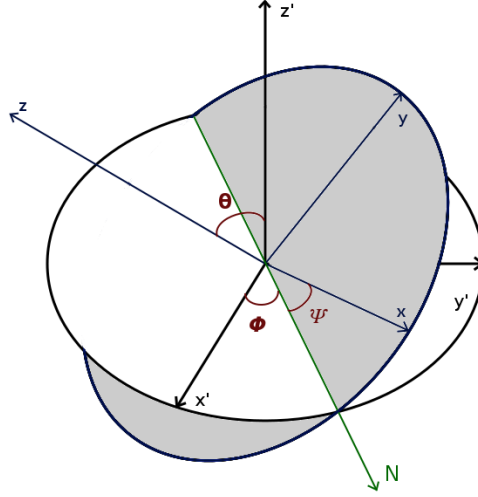


Figure 1: Euler Angles. We see two coordinate system  $S(x, y, z)$  and  $S'(x', y', z')$  and Euler angles together with the line of nodes, shown by  $N$ .  $\theta$  is the angle between  $z'$ -axis and  $z$ -axis,  $\phi$  is the angle between  $x'$ -axis and the line of nodes, and  $\psi$  is the angle between the line of nodes and  $x$ -axis.

It is customary to define domain of these angles as;  $0 < \theta < \pi$ ,  $0 < \phi < 2\pi$  and  $0 < \psi < 2\pi$ . However, in some cases different domains can be used.

By using Euler angles, angular velocities of rotating rigid bodies can be defined as;  $\dot{\theta}$ ,  $\dot{\phi}$  and  $\dot{\psi}$ .  $\dot{\theta}$  is shown in the direction of the line of nodes,  $\dot{\phi}$  is shown in the direction of  $\hat{z}'$ , and  $\dot{\psi}$  is shown in the direction of  $\hat{z}$ . Then the angular velocities in body coordinate system are

$$\begin{aligned} w_x &= \dot{\theta} \cos \psi + \dot{\phi} \sin \theta \sin \psi \\ w_y &= -\dot{\theta} \sin \psi + \dot{\phi} \sin \theta \cos \psi \\ w_z &= \dot{\psi} + \dot{\phi} \cos \theta. \end{aligned} \tag{1}$$

These angular velocities can be used to define rotations of rigid bodies in the body coordinate system. We need to mention that these three angles are not linearly independent of each other since  $z$  and  $z'$  axes are not perpendicular to each other. Some of the complicated structure of rigid body rotations are related to this structure. Though this complicated structure, they are very successful.

The motion of a symmetric top can also be studied in terms of these angular velocities, Eq. (1). A symmetric top can be considered as child's top having rotational symmetry in one axis, but in general, any object having such symmetry can be studied with below techniques.

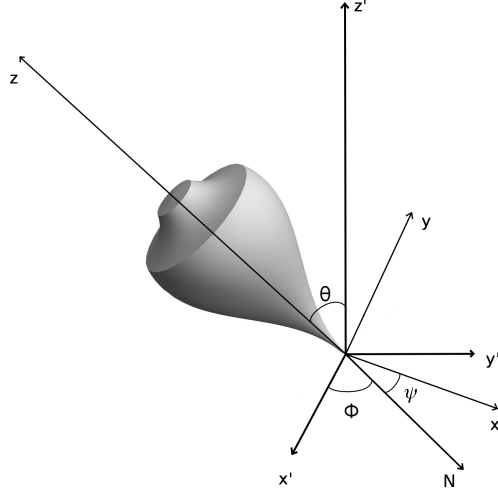


Figure 2: Symmetric top and Euler angles. Primed letters represent axes of the stationary reference frame, ordinary letters represent axes of the body reference frame.

The main property of the symmetric top is related to moments of inertia, i.e.  $I_x = I_y \neq I_z$ . For the child's top, Fig. 2,  $I_z > I_x$ ; and for cigar shaped structures  $I_z < I_x$ . We see a symmetric top in Fig. 2, its symmetry axis is chosen as  $z$ -axis and when we mention about symmetric top, mostly we consider that it spins around that axis. For the case shown in the figure, the fixed point is the tip of the symmetric top, the origin of both reference systems. The body coordinates,  $S(x, y, z)$ , are fixed on symmetric top and rotates with it. Euler angles are also shown in the figure. To define the motion of the symmetric top, we need to use 7 variables;  $\theta, \phi, \psi, \dot{\theta}, \dot{\phi}, \dot{\psi}$  and  $t$ . As symmetric top spins  $\psi$  changes, and the gravitational force causes changes in  $\theta$ , the change of  $\theta$  causes changes in  $\phi$ . There are many interesting cases related to the motion of the symmetric top and we will explain these below.

## 2.2 Methods

To study the symmetric top problem, one needs equations of motion, which can be written directly from Euler equations or can be obtained from Lagrangian. Firstly, we will give the application of Euler equations to the symmetric top problem and then we will obtain the same equations from Lagrangian and energy.

### 2.2.1 Euler equations

If we apply a force to a rigid body with a fixed point, then that rigid body can rotate. The torque, cause of the angular acceleration, is defined as

$$\vec{\tau} = \vec{r} \times \vec{F} \quad (2)$$

where  $\vec{F}$  is the force, and  $\vec{r}$  is the vector representing the distance from the rigid body's fixed point to the acting point of the force.

If there is a torque applied to a rigid body, as time changes there will be a change in the angular momentum,  $\vec{L} = I\vec{\omega}$  where  $I$  is the moment of inertia tensor. In the stationary reference frame, the relation between torque and angular momentum can be written as

$$\frac{d\vec{L}'}{dt} = \vec{\tau}'. \quad (3)$$

While writing this equation in the body reference frame, we should take into account that it is a non-inertial reference frame. In a rotating reference frame, here it is the body coordinate system, we should consider the effects of rotations and they will result in an additional term,  $\vec{\omega} \times$ , to the time derivative,  $(\frac{d}{dt})_{S'} = (\frac{d}{dt})_S + \vec{\omega} \times$ . Then, in the body coordinate system Eq. (3) becomes

$$\frac{d\vec{L}}{dt} + \vec{\omega} \times \vec{L} = \vec{\tau} \quad (4)$$

Here we have an extra term,  $\vec{\omega} \times \vec{L}$ , which is the key to understanding rigid body rotations. This extra term acts like torque in the body coordinate system. We can write components of Eq. (4) in the body coordinate system

as

$$\begin{aligned}
\tau_x &= I_x \dot{w}_x - (I_y - I_z) w_y w_z \\
\tau_y &= I_y \dot{w}_y - (I_z - I_x) w_x w_z \\
\tau_z &= I_z \dot{w}_z - (I_x - I_y) w_x w_y
\end{aligned} \tag{5}$$

where  $I_i$ 's are corresponding moments of inertia and  $w_i$ 's are angular velocities given in Eq. (1). Equations in Eq. (5) are Euler equations for a rotating rigid body in the body reference frame, and they correspond to equations of motion for them. The left-hand side of these equations corresponds the relevantly applied torque, the first term at the right-hand side is angular acceleration times moment of inertia in the considered direction and the second term corresponds to the inertial torque arising from being non-inertial reference frame. Euler equations are written in the traditional way in Eq. (5), however, taking the second term to the left-hand side may help to understand in a better way. In that case, we can write Euler equations as

$$\begin{aligned}
\tau_x + (I_y - I_z) w_y w_z &= I_x \dot{w}_x \\
\tau_y + (I_z - I_x) w_x w_z &= I_y \dot{w}_y \\
\tau_z + (I_x - I_y) w_x w_y &= I_z \dot{w}_z.
\end{aligned} \tag{6}$$

Now, terms at the left-hand side correspond to the torque, felt by the rigid body, and the terms at the right-hand side are angular acceleration times moment of inertia.

Now, we will consider a symmetric top and write Euler equations for that symmetric top under the influence of the gravitational field. In the body reference frame, the torque caused by the gravitational force is

$$\begin{aligned}
\vec{\tau} &= \vec{r} \times \vec{F} \\
&= Mgl \sin \theta (\cos \psi \hat{x} - \sin \psi \hat{y})
\end{aligned} \tag{7}$$

where  $l$  is the distance from the fixed point to the center of mass and  $M$  is mass of the rigid body. The direction of this torque is in the direction of the line of nodes. If there is not any initial angular momentum, then the torque will only cause an angular acceleration in the direction of lines of nodes,  $\ddot{\theta}$ , and the motion will be like a pendulum. If there is an initial angular momentum the motion will be complex and other components of the angular momentum will also change. This complex system is defined by

Euler equations. One may consider that in such a case we can use inertial reference frame to avoid such complications, however in that case complexity will show itself in another place, and moments of inertia will be much more complex and resulting equations will be same. In one way or another way we need to deal with this complex system.

If we insert the torque arising from the gravitational interaction in Eq. (6) and use angular velocities in terms of Euler angles in the case of a symmetric top, we obtain Euler equations for that symmetric top as

$$Mgl \sin \theta \cos \psi + (I_x - I_z)(\dot{\psi} + \dot{\phi} \cos \theta)(-\dot{\theta} \sin \psi + \dot{\phi} \sin \theta \cos \psi) \quad (8)$$

$$= I_x(\ddot{\theta} \cos \psi - \dot{\theta} \dot{\psi} \sin \psi + \ddot{\phi} \sin \theta \sin \psi + \dot{\phi} \dot{\theta} \cos \theta \sin \psi + \dot{\phi} \dot{\psi} \sin \theta \cos \psi),$$

$$-Mgl \sin \theta \sin \psi + (I_z - I_x)(\dot{\psi} + \dot{\phi} \cos \theta)(\dot{\theta} \cos \psi + \dot{\phi} \sin \theta \sin \psi) \quad (9)$$

$$= I_x(-\ddot{\theta} \sin \psi - \dot{\theta} \dot{\psi} \cos \psi + \ddot{\phi} \sin \theta \cos \psi + \dot{\phi} \dot{\theta} \cos \theta \cos \psi - \dot{\phi} \dot{\psi} \sin \theta \sin \psi),$$

$$0 = I_z(\ddot{\psi} + \ddot{\phi} \cos \theta - \dot{\phi} \dot{\theta} \sin \theta). \quad (10)$$

Now, we need to make the necessary simplifications to be able to analyze motion. Eq. (10) is obtained from  $I_z \dot{w}_z$  and it is equal to zero, as it is seen from the equation. From this equation, we can conclude that  $I_z w_z$  is constant, and we can write it in terms of another constant  $a$  as

$$I_x a = I_z(\dot{\psi} + \dot{\phi} \cos \theta). \quad (11)$$

This constant is chosen in this way by considering future simplifications.

Multiplying Eq. (8) with  $\sin \psi$  and Eq. (9) with  $\cos \psi$  and adding them we obtain

$$\ddot{\phi} = \frac{\dot{\theta}}{\sin \theta} \left( -2\dot{\phi} \cos \theta + \frac{I_z}{I_x}(\dot{\psi} + \dot{\phi} \cos \theta) \right). \quad (12)$$

We can write this in terms of  $a$  as

$$\ddot{\phi} = \frac{\dot{\theta}}{\sin \theta} (-2\dot{\phi} \cos \theta + a). \quad (13)$$

We can multiply it by  $\sin^2 \theta$  and we can write it as a total time derivative

$$\frac{d}{dt} \left[ \dot{\phi} \sin^2 \theta + a \cos \theta \right] = 0. \quad (14)$$

Since this total time derivative is equal to zero, the term inside the parenthesis is equal to another constant

$$b = \dot{\phi} \sin^2 \theta + a \cos \theta. \quad (15)$$

By using constants  $a$  and  $b$ , we can write Eq. (13) as

$$\ddot{\phi} = \frac{\dot{\theta}}{\sin \theta} \left( -2 \frac{b - a \cos \theta}{\sin^2 \theta} \cos \theta + a \right). \quad (16)$$

Also multiplying Eq. (8) with  $\cos \psi$  and Eq. (9) with  $\sin \psi$  and subtracting the first one from the second we obtain

$$\ddot{\theta} = \sin \theta \left( \frac{Mgl}{I_x} + \dot{\phi}^2 \cos \theta - \frac{I_z}{I_x} \dot{\phi}(\dot{\psi} + \dot{\phi} \cos \theta) \right). \quad (17)$$

We can rewrite this equation in terms of the defined constants as

$$\ddot{\theta} = \sin \theta \left( \frac{Mgl}{I_x} + \left( \frac{b - a \cos \theta}{\sin^2 \theta} \right)^2 \cos \theta - a \frac{b - a \cos \theta}{\sin^2 \theta} \right). \quad (18)$$

We can also find  $\ddot{\psi}$  by using Eq. (12) in Eq. (10) as

$$\ddot{\psi} = -\cot \theta \dot{\theta} \left[ \frac{I_z}{I_x} (\dot{\psi} + \dot{\phi} \cos \theta) - 2\dot{\phi} \cos \theta \right] + \dot{\phi} \dot{\theta} \sin \theta, \quad (19)$$

and we can write this equation in terms of constants as

$$\ddot{\psi} = \dot{\theta} \left[ -a \cot \theta + \frac{b - a \cos \theta}{\sin^3 \theta} (1 + \cos^2 \theta) \right]. \quad (20)$$

We obtained the three angular accelerations from Euler equations in two ways. In one case Eq.s (12), (17) and (19), they are obtained in terms of  $\theta$  and angular velocities. In the other case Eq.s (16), (18) and (20), they are obtained in terms of  $\theta$ ,  $\dot{\theta}$  and constants of motion  $a$  and  $b$ .

We can also get  $\dot{\theta}$  in terms of constants of motion. We can multiply Eq.(17) by  $2\dot{\theta}$  and Eq.(12) by  $2\dot{\phi} \sin^2 \theta$  and add these to get

$$2\dot{\theta}\ddot{\theta} + 2\dot{\phi}\ddot{\phi}\sin^2 \theta + 2\dot{\theta}\dot{\phi}^2 \sin \theta \cos \theta - 2\frac{Mgl}{I_x}\dot{\theta} \sin \theta = 0. \quad (21)$$

The left-hand side of this equation can also be written as a total time derivative

$$\frac{d}{dt} \left[ \dot{\theta}^2 + \dot{\phi}^2 \sin^2 \theta + 2\frac{Mgl}{I_x} \cos \theta \right] = 0. \quad (22)$$



This gives us another constant and by multiplying it with  $I_x/2$ , we can define it as

$$E' = \frac{I_x}{2} \dot{\theta}^2 + \frac{I_x}{2} \dot{\phi}^2 \sin^2 \theta + Mgl \cos \theta, \quad (23)$$

or

$$E' = \frac{I_x}{2} \dot{\theta}^2 + \frac{I_x}{2} \frac{(b - a \cos \theta)^2}{\sin^2 \theta} + Mgl \cos \theta \quad (23')$$

and if we add another constant,  $a^2 I_x^2 / (2I_z)$ , we will get the energy as a result.

We can write  $\dot{\theta}^2$  from Eq. (23') as

$$\dot{\theta}^2 = \frac{2E'}{I_x} - \frac{(b - a \cos \theta)^2}{\sin^2 \theta} - \frac{2Mgl}{I_x} \cos \theta. \quad (24)$$

As it is seen,  $\dot{\theta}$  is also obtained in terms of constants of motion. Then we can obtain all angular accelerations in terms of constants of motion ( $a$ ,  $b$  and  $E'$  or  $E$ ) and as functions of  $\theta$ . We have mentioned that there are 7 variables to define this system, 3 of them ( $\phi$ ,  $\psi$  and  $t$ ) are not available in the angular accelerations, then we left with 4 variables ( $\theta$ ,  $\dot{\theta}$ ,  $\dot{\phi}$  and  $\dot{\psi}$ ) in equations giving angular accelerations. Equations giving angular accelerations correspond to the equations of motion since these three variables are not available in angular acceleration equations then the system should be symmetric with respect to these; there are some quantities that do not change as these variables change. According to Noether's theorem, we should have three constants of motion. We already obtained these;  $E'$  or  $E$  corresponds to conservation of energy and related to  $t$  symmetry,  $a$  corresponds to conservation of angular momentum in  $z$ -direction and related to  $\psi$  symmetry, and  $b$  corresponds to the conservation of angular momentum in  $z'$ -direction and related to  $\phi$  symmetry.

These constants of the motion can be determined by the initial values;  $\theta_0$ ,  $\dot{\theta}_0$ ,  $\dot{\phi}_0$  and  $\dot{\psi}_0$ . After determining these constants we can get angular accelerations in terms of these constants, and then angular accelerations depend on only one variable  $\theta$ . We do not have to use angular accelerations to get necessary information on the system. By using constants of motion, i.e. Eq. (11) and Eq. (15), we can get angular velocities  $\dot{\phi}$  and  $\dot{\psi}$  as

$$\dot{\phi} = \frac{b - a \cos \theta}{\sin^2 \theta} \quad (25)$$

and

$$\dot{\psi} = \frac{I_x}{I_z} a - \frac{b - a \cos \theta}{\sin^2 \theta} \cos \theta. \quad (26)$$

These equations together with Eq. (24) show that all angular velocities and accelerations can be obtained in terms of constants of motion ( $a$ ,  $b$  and  $E'$ ) and as functions of  $\theta$ . Hence, we can say that if we are able to find  $\theta(t)$ , we can find all other variables as functions of  $t$ .

Now, we should focus on  $\theta$ . Its change is given by  $\dot{\theta}$ , Eq. (24). We see that  $\dot{\theta}$  is a function of  $\theta$  and it is obtained as a square and we need to take the square root to get it. From Eq. (24), we can say that the right-hand side of it should be positive for physical motion. The solution of Eq. (24) is in terms of elliptic integrals. Without entering its mathematical details, we can comment on motion without finding the solution of Eq. (24). If we consider the second term in Eq. (24), we see that it goes to negative infinity as  $\theta$  goes to 0 or  $\pi$ . Then, the right-hand side of this equation can be positive only for an interval. The first term, which should be calculated by using Eq. (23) from the initial values and corresponds to energy, determines that interval mainly. We can also say that for each  $\theta$  value making the right-hand side positive,  $\dot{\theta}$  can be positive or negative. On the other hand  $\dot{\phi}$  and  $\dot{\psi}$  can get only one value for each  $\theta$  value. This is related to the motion of the symmetric top, which will be clear in the next sections.

We should also mention that if  $\theta$  is greater than  $\pi/2$ , then there is a possibility that  $E'$  can be negative. This is related to the definition of the origin. We should also keep in mind that  $E'$  is not the energy, it gives energy only if we add another constant related to the spin.

We have seen that angular velocities and accelerations can be written in terms of constants of the motion. Then, we can use two different set to define the motion of the symmetric top;  $\theta$  and angular velocities or  $\theta$  and constants of the motion. Both sets are equivalent and they define the motion of the symmetric top. We will use both to analyze the motion.

One can obtain variables ( $\theta$ ,  $\phi$  and  $\psi$ ) to describe the motion of the symmetric top in two different ways. The first way is to find  $\theta(t)$  from Eq. (24) and find angular velocities by using it and get  $\dot{\psi}(t)$  and  $\dot{\phi}(t)$ . The second way is solving angular accelerations Eq.s (12), (17) and (19). We will use both, however, we will not get  $\dot{\psi}(t)$  and  $\dot{\phi}(t)$  from the first technique. We will use numerical techniques in both. We will consider different possibilities in the following sections.

### 2.2.2 Lagrangian and Energy

Now, we will obtain the equations derived in the previous section from Lagrangian and energy.

For a spinning symmetric top with a fixed point, the kinetic energy is the total of kinetic energies due to all angular velocities

$$T = I_x w_x^2 + I_x w_y^2 + I_z w_z^2 \quad (27)$$

and under the gravitational field, the potential energy is

$$U = Mgl \cos \theta. \quad (28)$$

Then, Lagrangian becomes

$$\begin{aligned} L &= T - U \\ &= \frac{I_x}{2}(\dot{\theta}^2 + \dot{\phi}^2 \sin^2 \theta) + \frac{I_z}{2}(\dot{\psi} + \dot{\phi} \cos \theta)^2 - Mgl \cos \theta. \end{aligned} \quad (29)$$

We can find equations of motion from this Lagrangian by using Euler-Lagrange equations,  $\frac{d}{dt} \left( \frac{\partial L}{\partial \dot{q}_i} \right) - \frac{\partial L}{\partial q_i} = 0$ . In this problem  $q_i$ 's correspond  $\psi$ ,  $\phi$  and  $\theta$ . There are two cyclic coordinates,  $\psi$  and  $\phi$ , and there should be two corresponding conserved angular momenta since they define rotations. One can obtain these conserved angular momenta from Euler-Lagrange equations for angular momenta in  $z$  and  $z'$  direction as

$$\begin{aligned} L_z &= I_z(\dot{\psi} + \dot{\phi} \cos \theta), \\ L_{z'} &= I_x \dot{\phi} \sin^2 \theta + I_z(\dot{\psi} + \dot{\phi} \cos \theta) \cos \theta. \end{aligned} \quad (30)$$

Using these conserved angular momenta, we can define following constants

$$\begin{aligned} a &= \frac{I_z(\dot{\psi} + \dot{\phi} \cos \theta)}{I_x}, \\ b &= \dot{\phi} \sin^2 \theta + \frac{I_z}{I_x}(\dot{\psi} + \dot{\phi} \cos \theta) \cos \theta \\ &= \dot{\phi} \sin^2 \theta + a \cos \theta. \end{aligned}$$

These are the same constants that are obtained in the previous section. As it is seen, these constants of motion are in the dimension of angular velocity.

$\dot{\phi}$  can be written in terms of them as

$$\dot{\phi} = \frac{b - a \cos \theta}{\sin^2 \theta} \quad (25)$$

and  $\dot{\psi}$  becomes

$$\dot{\psi} = \frac{I_x}{I_z} a - \frac{b - a \cos \theta}{\sin^2 \theta} \cos \theta. \quad (26)$$

There is another variable in Lagrangian,  $\theta$ , and corresponding Euler-Lagrange equation can be found as

$$\ddot{\theta} = \sin \theta \left[ \frac{Mgl}{I_x} + \dot{\phi}^2 \cos \theta - \frac{I_z}{I_x} \dot{\phi}^2 \cos \theta - \frac{I_z}{I_x} \dot{\phi} \dot{\psi} \right]. \quad (17)$$

These equations are the same as the ones in the previous section. If we write the angular velocities in terms of constants in Eq. (17), then we obtain Eq. (18).

We can also find other angular accelerations by taking the time derivative of Eq.s (25) and (26) as

$$\ddot{\phi} = \frac{\dot{\theta}}{\sin \theta} \left( a - 2 \frac{b - a \cos \theta}{\sin^2 \theta} \cos \theta \right), \quad (16)$$

and

$$\ddot{\psi} = \frac{\dot{\theta}}{\sin^3 \theta} (b + b \cos^2 \theta - 2a \cos \theta). \quad (20)$$

These equations are also the same as the previously obtained ones. If we write  $a$  and  $b$  in terms of angular velocities then we obtain Eq.s (12) and (19).

We can also obtain  $\theta$  by using the energy. Since we are considering dissipation free cases, there is another conserved quantity in the motion, energy. We can also see conservation of energy from the independence of kinetic energy and potential energy from time. Energy is the total of the kinetic energy and potential energy,  $E = T + U$ , and for the symmetric top it is

$$E = \frac{I_x}{2} (\dot{\theta}^2 + \dot{\phi}^2 \sin^2 \theta) + \frac{I_z}{2} (\dot{\psi} + \dot{\phi} \cos \theta)^2 + Mgl \cos \theta. \quad (31)$$

From the definition of  $a$ , we see that the second term is constant and by subtracting it from the energy we obtain another constant

$$E' = \frac{I_x}{2} \dot{\theta}^2 + \frac{I_x}{2} \frac{(b - a \cos \theta)^2}{\sin^2 \theta} + Mgl \cos \theta. \quad (23')$$

This is the same constant that we obtained previously. If we take the total time derivative of  $E'$  by considering it depends on  $\theta$  and  $\dot{\theta}$ , by equating it to zero we obtain Eq. (18).

If we change variable by using  $u = \cos \theta$ , from Eq. (23') we obtain

$$\dot{u}^2 = (1 - u^2)(\alpha - \beta u) - (b - au)^2, \quad (32)$$

where  $\alpha = 2E'/I_x$  and  $\beta = 2Mgl/I_x$ . We can take the square root of both sides and obtain time as an integral of  $u$

$$t = \int \frac{du}{\sqrt{(\alpha - \beta u)(1 - u^2) - (b - au)^2}}. \quad (33)$$

This kind of integrals are known as elliptic integrals, and again we encountered with them and we will not deal with details of these integrals as we did in the previous section. We will do this integration numerically, and then we will get  $t$  for different  $u$  values, and using this result it is possible to obtain  $\theta$  for different  $t$ . After obtaining  $\theta$ , one can obtain  $\dot{\theta}$ ,  $\dot{\phi}$  and  $\dot{\psi}$  by using Eq.s (23), (25) and (26) and also  $\phi$  and  $\psi$  by using them. However, obtaining  $\phi$  and  $\psi$  from these can be cumbersome due to not evenly spaced time.

Without finding the solution of the equation, it is possible to make some comments on the motion using Eq. (32). Firstly let us call the right-hand side of Eq. (32) as  $f(u)$

$$f(u) = (1 - u^2)(\alpha - \beta u) - (b - au)^2. \quad (34)$$

Since  $u = \cos \theta$ , the time derivative of  $u$  corresponds  $\dot{\theta}$ . Then, the roots of  $f(u)$  correspond to  $\dot{\theta} = 0$ . For the motion of the symmetric top, the domain of  $\theta$  can be considered as  $[0, \pi]$  and then  $u$  can take values  $-1 \leq u \leq 1$ .

$f(u)$  can have three roots since it is a cubic function. Two of the roots correspond to turning angles of  $\theta$ . The third one is irrelevant from the physical motion of the symmetric top.  $u$  and constants of the motion can also be used to analyze the motion of the symmetric top.

### 3 Motion of a spinning symmetric top

We have seen that we have an extra term in the Euler equations,  $\vec{w} \times \vec{L}$ . It is related to the symmetric top's being non-inertial reference frame. For the symmetric top, angular velocity and angular momentum can be in different

directions. These two things make harder to understand the motion of the symmetric top from torque and angular momentum. Here, we will solve Euler equations for the symmetric top numerically and explain its motion from these solutions.

We have seen that we can use two equivalent set to study motion;  $E'$ ,  $b$ ,  $a$  and  $u$  (or  $\theta$ ) or  $\dot{\phi}$ ,  $\dot{\psi}$ ,  $\dot{\theta}$  and  $\theta$ . By using  $\dot{\phi}_0$ ,  $\dot{\psi}_0$  and  $\theta_0$  we can determine  $b$  and  $a$ , and including  $\dot{\theta}_0$  we can determine  $E'$ . We mentioned that these three constants  $E'$ ,  $b$  and  $a$  correspond to conservation of energy, the conservation of the angular momentum in  $z$  direction and the conservation of the angular momentum in  $z'$  direction respectively. Both sets have their own advantages; the first set provides advantages to understand the motion in terms of conserved quantities and provides insight, and the second one provides advantages to study the motion dynamically. In this work, we will use them in a mixed way to understand the motion.

Let us consider a symmetric top with moments of inertia  $I_x$  and  $I_z$ , mass  $M$ , the distance from tip to center of mass  $l$ , and also consider that this symmetric top spins with some initial angular velocity  $\dot{\psi}_0$  and started to its motion with an initial inclination  $\theta_0$ . It can also have initial angular velocities  $\dot{\phi}_0$  and  $\dot{\theta}_0$ ; even if  $\dot{\phi}_0$  and  $\dot{\theta}_0$  are zero at the beginning, they can be developed during the motion. Precession is related to  $\dot{\phi}$  and nutation is related to  $\dot{\theta}$ . There are different types of motion for the symmetric top. These can be obtained from different initial values and can be understood from the constants of the motion.

It is easier to consider the motion of the symmetric top with the constants of motion.  $E'$  can be used to understand the changes in  $\theta$  and  $\dot{\theta}$ .  $a$  and  $b$  can be used to understand changes in  $\dot{\psi}$  and  $\dot{\phi}$  according to changes in  $\theta$ .  $\dot{\psi}$  and  $\dot{\phi}$  are not linearly independent of each other, then  $a$  and  $b$  are entangled. Though this entangled structure, they provide the necessary information to understand the motion. By using changes in  $\theta$ , we can understand changes in  $\dot{\phi}$  mainly from  $b$  and in  $\dot{\psi}$  mainly from  $a$ . We can also use Eq.s (25) and (26) to understand these changes.

In some places  $f(u)$  is used to consider the motion of the symmetric top in  $\theta$ , however, it is hard to imagine the symmetric top's motion in terms of  $u$ . It is also possible to use an effective potential to analyze the motion in  $\theta$ , and it is much more convenient for interpretation.

We will mainly use the effective potential to understand some parts of the motion, but we will also consider  $f(u)$  for comparison. By considering Eq.

(23') and using  $E' = I_x \dot{\theta}^2/2 + U_{eff}$ , the effective potential can be written as

$$U_{eff}(\theta) = \frac{I_x}{2} \frac{(b - a \cos \theta)^2}{\sin^2 \theta} + Mgl \cos \theta. \quad (35)$$

It is seen that  $U_{eff}$  depends only one variable  $\theta$ . One may consider that only changes in  $\theta$  will effect  $\dot{\theta}$ , but this is not true since all things are coupled, and these coupled variables affect each other obeying conservation of energy and angular momenta. It can be seen from Eq. (18) that change in  $\theta$  is more complex.

This effective potential will go to infinity at the domain boundaries of  $\theta$ ,  $[0, \pi]$ , and have a minimum within these limits. Then, the form of the potential is like a well. We see the general structure of the  $U_{eff}$  in Fig. 3. The minimum of the effective potential can be negative and depends on  $I_x$ ,  $Mgl$ ,  $b$  and  $a$ .

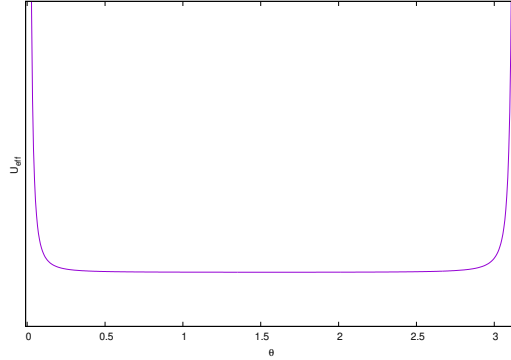


Figure 3: General form of  $U_{eff}$  for  $0 < \theta < \pi$ .

Firstly, let us consider the motion from the effective potential and start with the denominator of the first term to understand different types of the motion; if  $\theta$  goes to 0 or  $\pi$ , the denominator approaches to zero and the first term goes to infinity.

By looking at these infinities, one can consider that the motion at  $\theta = 0$  or  $\pi$  is not possible, however, it is possible. If at the beginning of the motion  $\theta_0$  is equal to 0 or  $\pi$  together with  $\dot{\theta}_0 = 0$ , then this configuration corresponds sleeping top and in these two cases the torque arising from the gravitational force on the symmetric top is equal to zero and the symmetric top will continue its spinning without any change in  $\theta$ .

There are different possibilities for  $E'$  with respect to the minimum of the effective potential and other things. These will result in different types of motion.

If  $E'$  is equal to the minimum of  $U_{eff}$ , then the right-hand side of Eq. (24) becomes equal to zero. Since the right-hand side can not be negative for the physical motion then only one  $\theta$  value is possible, and  $\dot{\theta}$  will be equal to zero throughout the motion. There are other things that should be considered for this type of motion, which we will consider later. This case will correspond to regular precession.

If  $E'$  is greater than the minimum value of  $U_{eff}$ . Then at two different values of  $\theta$ ,  $U_{eff}$  will be equal to  $E'$ . These two different  $\theta$  values correspond to the turning angles of the symmetric top. Since  $\theta$  will change between these two turning angles periodically,  $\dot{\theta}$  should be either positive or negative at different parts of the period. As  $\theta$  changes between these two turning angles,  $\dot{\phi}$  will have different values and these values will identify the type of motion.

To understand different possibilities for  $\dot{\phi}$ , we will consider  $\dot{\phi}$  in terms of constants of motion and  $\theta$ ;

$$\dot{\phi} = \frac{b - a \cos \theta}{\sin^2 \theta}. \quad (25)$$

We already considered cases making denominator zero, they were giving infinities for  $U_{eff}$ . The nominator can be zero, greater than zero or less than zero, dependently  $\dot{\phi}$  will have the same properties. These three possibilities together with  $E'$  and  $U_{eff}$  relation will result in different types of motion. There will be changes in the angular velocity  $\dot{\psi}$  as well. It will change as  $\dot{\phi}$  changes according to the constant  $a$  and  $b$ . We will analyze these changes for different types of motion.

We have mentioned that calculations of  $\phi$  and  $\psi$  can be cumbersome from the previously mentioned method, i.e. using the integration of Eq. (33). There is another method that we can calculate variables of the motion: numerical solutions of the angular accelerations. In this numerical solution, the cumbersome structure is not present and it is preferable. However, solving with only one method can sometimes lead problems. When we solve from two different methods, we obtain a checking point for calculations. Then we will follow such a structure and calculate from both techniques. We will not calculate  $\phi$  and  $\psi$  from the first technique since if  $\dot{\phi}$  and  $\dot{\psi}$  calculations



are consistent there will be no need to deal with an unevenly spaced time interval.

We will solve following angular accelerations

$$\begin{aligned}\ddot{\theta} &= \sin \theta \left[ \frac{Mgl}{I_x} + \dot{\phi}^2 \cos \theta - \frac{I_z}{I_x} \dot{\phi}^2 \cos \theta - \frac{I_z}{I_x} \dot{\phi} \dot{\psi} \right] \\ \ddot{\phi} &= \frac{\dot{\theta}}{I_x \sin \theta} \left[ I_z \dot{\psi} + I_z \dot{\phi} \cos \theta - 2I_x \dot{\phi} \cos \theta \right] \\ \ddot{\psi} &= -\cot \theta \left[ \frac{I_z}{I_x} \dot{\theta} \dot{\psi} + \frac{I_z}{I_x} \dot{\theta} \dot{\phi} \cos \theta - 2\dot{\theta} \dot{\phi} \cos \theta \right] + \dot{\theta} \dot{\phi} \sin \theta\end{aligned}$$

by integrating numerically. Since they are all coupled, we will integrate them in a coupled way to get the solution. For all cases we will take  $\phi_0 = 0$  and  $\psi_0 = 0$ . We will obtain three angles and three angular velocities as a function of time from this technique. Then we will plot three-dimensional figures, and these plots will give more insight into the motion. Remaining plots related to  $\theta$ ,  $\phi$ ,  $\psi$ ,  $\dot{\theta}$ ,  $\dot{\phi}$  and  $\dot{\psi}$  will be available at the appendix. All results given below are consistent in  $\theta$ ,  $\dot{\theta}$ ,  $\dot{\phi}$  and  $\dot{\psi}$  for two techniques.

Now let us overview of the motion of the symmetric top to understand these three-dimensional figures;  $\psi$  will be related to rotation around symmetry axis,  $\theta$  and  $\phi$  will be related to the motion of the symmetry axis. If we plot the points defined by  $\theta$  and  $\phi$ , obtained from equations describing the motion of the symmetric top, in three-dimensional way, we will get the intersection of the unit sphere having the origin at the tip of the symmetric top with the symmetry axis of the symmetric top. So, these three-dimensional figures correspond to the motion of the symmetry axis. These type drawings are known as the locus of the figure (symmetry) axis on the unit sphere.

We need to mention another point about the first method. At the turning angles of  $\theta$  there are some discontinuities, arising from the separation of the integration as increasing and decreasing part. This separation causes loss of some information, decreasing integration step to smaller values will be helpful.

### 3.1 Sleeping top

Sleeping top is a case that the symmetric top continues its spinning with initial  $\psi_0$  without changing its orientation. There are two possible  $\theta$  values for the sleeping top; 0 and  $\pi$ . To obtain such a motion, it is enough to let the

symmetric top spin along  $z'$  or  $-z'$  axis without any initial  $\dot{\theta}$ . In these cases, the symmetric top continues its spinning without changing its orientation.

Let us consider the denominator of Eq. (25), if  $\theta$  is equal to 0 or  $\pi$ , it becomes zero and gives infinities. These infinities do not mean that  $\dot{\phi}$  becomes infinite, it shows that  $\dot{\phi}$  can be irrelevant for the motion in these cases.

In the sleeping top case, body  $z$ -axis becomes parallel or anti-parallel to the stationary  $z'$ -axis, and  $\dot{\phi}$  becomes irrelevant for the motion since it defines how body  $z$ -axis rotates around stationary  $z'$ -axis. To obtain equations describing such a case one needs to rearrange terms with  $\dot{\phi}$ . If  $\dot{\phi}$  is not eliminated from the relevant equations, there can be some misleading situations.

If  $\theta_0 = 0$  then  $z$ -axis overlaps with  $z'$ -axis. As we mentioned previously we should eliminate terms with  $\dot{\phi}$  from the equations. After eliminating  $\dot{\phi}$  from the relevant equations and letting  $\theta = 0$ , from Eq.s (30) we see that  $L_z$  becomes equal to  $L'_z$ . Then from Eq. (17), we see that the angular acceleration  $\ddot{\theta}$  is equal to zero. If  $\theta_0 = \pi$ , then  $z$ -axis overlaps with negative  $z'$ -axis and we get  $L_z = -L'_z$ . Again  $\ddot{\theta}$  becomes zero. Since  $\dot{\theta}_0 = 0$  and  $\ddot{\theta} = 0$ , there will be no change in  $\theta$ .

In these two cases, the torque arising from the gravitational force on the symmetric top is equal to zero and the symmetric top will continue its spinning without any change in  $\theta$ . Here we are considering dissipation free cases, then the spin angular momentum arising from  $\dot{\psi}$  does not decay.

In daily life, for the spinning symmetric top, there is always friction and this friction causes decay of  $\dot{\psi}$ . However, this is not the reason for falling off the symmetric top. If the symmetric top's symmetry axis is parallel to stationary  $z'$ -axis which is the direction of gravitational force then torque will be always zero and the symmetric top will not change its orientation. The reason of the change in the orientation of the symmetric top is small fluctuations in the direction of the symmetric top, any small change independent of the amount will cause torque and this will trigger motions different than sleeping top. We will later give some more explanations for such cases.

### 3.2 Regular precession

The regular precession is the precession that  $\theta$  does not change and  $\dot{\phi}$  is constant. For the regular precession, the spinning symmetric top should start its motion with an initial inclination  $\theta_0$  and angular velocity  $\dot{\phi}_0$  and

continue its precession without nutation,  $\dot{\theta}_0 = 0$ . We can find such values by using the effective potential.

If  $E'$  is equal to the minimum of  $U_{eff}$ , then only one  $\theta$  value is possible. Since  $\theta$  does not change,  $\dot{\theta}$  is always zero. To find initial values for such a configuration, we can take the derivative of  $U_{eff}$

$$\frac{dU_{eff}(\theta)}{d\theta} = \frac{I_x}{2} \left( \frac{2(b - a \cos \theta)a \sin \theta}{\sin^2 \theta} - \frac{2(b - a \cos \theta)^2 \cos \theta}{\sin^3 \theta} \right) - Mgl \sin \theta \quad (36)$$

and then equate it to the zero. We can write this equation after inserting  $b$  and  $a$  in terms of  $\dot{\phi}$  and  $\dot{\psi}$  as

$$(\dot{\phi}^2 \cos \theta (I_z - I_x) + \dot{\phi} \dot{\psi} I_z - Mgl) \sin \theta = 0. \quad (37)$$

Here  $\sin \theta$  is a common multiplier and it is zero when  $\theta$  equals to 0 or  $\pi$ , which correspond sleeping top. We will look at the cases which makes the terms in the parenthesis equal to zero.

If we eliminate  $\sin \theta$ , we get

$$\dot{\phi}^2 \cos \theta (I_z - I_x) + \dot{\phi} \dot{\psi} I_z - Mgl = 0. \quad (38)$$

The discriminant of this equation is  $D = (I_z \dot{\psi})^2 + 4(I_z - I_x)Mgl \cos \theta$ . If  $4(I_z - I_x)Mgl \cos \theta = -(I_z \dot{\psi})^2$  then the discriminant will be equal to zero and only one  $\dot{\phi}$  will give regular precession. Since  $(I_z \dot{\psi})^2$  is always positive, the left-hand side should be negative for equality. If  $I_z < I_x$ , then  $\theta$  should be between 0 and  $\pi/2$ ; if  $I_z > I_x$ , then  $\theta$  should be between  $\pi/2$  and  $\pi$ , otherwise regular precession with one  $\dot{\phi}$  is not possible. Since the maximum value of  $|\cos \theta| = 1$ , then for regular precession with single  $\dot{\phi}$ , the spin angular velocity  $\dot{\psi}$  should be smaller than  $\sqrt{4Mgl|I_z - I_x|/I_z^2}$ . We will use the angular velocity  $\sqrt{4Mgl|I_z - I_x|/I_z^2}$  to discriminate regular precessions with single  $\dot{\phi}$  and two  $\dot{\phi}$  and designate it with  $\tilde{w}$ . Since  $\tilde{w}$  corresponds small angular velocities we will name symmetric tops spinning with smaller angular velocity than  $\tilde{w}$  as "weak top". If  $\dot{\psi} > \tilde{w}$ , then we will use "strong top" definition.

We can write Eq. (38) as

$$\dot{\phi}^2 \cos \theta - \dot{\phi} a + \frac{Mgl}{I_x} = 0. \quad (39)$$

We see that the discriminant will be equal to  $a^2 - 4Mgl \cos \theta / I_x$ . If  $a^2 < 4Mgl / I_x$ , then  $\theta$  should be between  $\pi/2$  and  $\pi$  to get regular precession. However, it is still possible to get regular precession when  $0 < \theta < \pi/2$ ,

which is mentioned previously when  $I_z < I_x$ . Using constant  $a$  makes harder to see these cases. On the other hand, if we use the previous relation it is easier to see them.

Still there are advantages of using  $a$ . We can also use  $\tilde{a} = \sqrt{4Mgl/I_x}$  to make discrimination for the symmetric top as "strong top" or "weak top". This is an approximation because of ignoring  $\cos \theta$ . If  $|a| > \tilde{a}$  the symmetric top will be designated as "strong top", and if  $|a| < \tilde{a}$  the symmetric top will be designated as "weak top". Both weak or strong top definitions are nearly the same, and either  $\dot{\psi}$  or  $a$  can be used to determine it. However, in some situations at the border, these definitions can conflict as a result of making approximations.

If we use Eq. (39), determination of  $\dot{\phi}$  and  $\dot{\psi}$  will not be as straightforward as Eq. (38), since constant  $a$  involves both. Here, we will use Eq. (38).

In regular precessions with single  $\dot{\phi}$  cases the relation between  $\theta$  and  $\dot{\psi}$  is

$$\cos \theta = -(I_z \dot{\psi})^2 / (4(I_z - I_x)Mgl). \quad (40)$$

The second possibility for regular precessions is obtained when the discriminant is positive. For a positive discriminant, giving regular precession for two  $\dot{\phi}$  value, roots can be obtained by using

$$\dot{\phi}_{1,2} = \frac{-I_z \dot{\psi} \pm \sqrt{D}}{2(I_z - I_x) \cos \theta}. \quad (41)$$

After assigning suitable values to  $\theta$  and  $\dot{\psi}$  for a symmetric top, from Eq. (41) it is possible to find  $\dot{\phi}$ , which will give a precession without nutation.

Now, we will obtain roots of Eq. (38) for different  $\dot{\psi}$  values. We will consider a symmetric top with parameters  $I_x = 0.00014 \text{ kgm}^2$ ,  $I_z = 0.00022 \text{ kgm}^2$  and  $Mgl = 0.068 \text{ J}$  for this and later calculations in this work. In this case  $\beta$  becomes 971.4. These parameters can correspond to the child's top or a symmetric top with disc-like structure, and gives  $\tilde{\omega} = 21.20 \text{ rad/s}$  and  $\tilde{a} = 44.08$ .

If we take  $\dot{\psi}$  equal to  $\sqrt{4Mgl(I_z - I_x)/I_z^2}$ , from Eq. (40) we obtain  $\theta$  as  $\pi$ , which corresponds to sleeping top and we can not obtain regular precession with single  $\dot{\phi}$ , then we need to take smaller  $\dot{\psi}$  values to obtain such a motion.

If we take  $\dot{\psi}$  as  $17 \text{ rad/s}$ , then we obtain  $\theta$  as  $2.269 \text{ rad}$  for the regular precession with single  $\dot{\phi}$ . In this case  $\dot{\phi}$  becomes  $36.36 \text{ rad/s}$ . For this case,  $U_{eff}$  is shown in Fig. 4. It is seen that  $E'$  intersects  $U_{eff}$  at its minimum, at

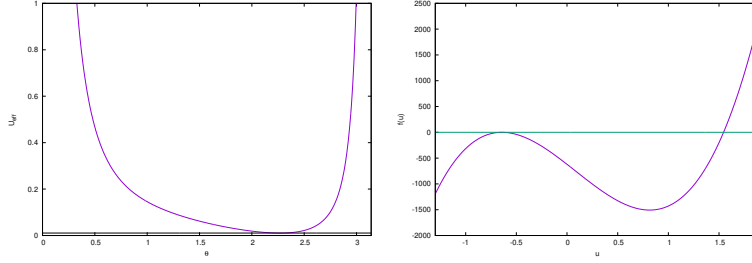


Figure 4:  $U_{eff}$  at left, and  $f(u)$  (the right-hand side of Eq. (32) as a function of  $u = \cos \theta$ ) at right.  $E'$  is plotted with straight black line in  $U_{eff}$  graph. This case gives regular precession with single  $\dot{\phi}$ , and initial values and constants of motion for this case as follows;  $\theta_0 = 2.269rad$ ,  $\dot{\theta}_0 = 0$ ,  $\dot{\psi}_0 = 17rad/s$ ,  $\dot{\phi} = 36.36rad/s$ ,  $E' = 0.01060J$ ,  $a = -10.02$ ,  $b = 27.78$  and  $\alpha = 151.2$ .

$\theta = 2.269rad$ . We see it also from  $f(u)$ ; it intersects with zero twice, and one of them gives regular precession,  $u = -0.6428$  corresponding  $\theta = 2.269rad$ .

If we choose  $\dot{\psi}$  greater than  $\tilde{w}$ , then we need to specify  $\theta$  as well to find  $\dot{\phi}$ . If we choose  $\dot{\psi} = 50rad/s$  and  $\theta = 1.1rad$ , then we obtain  $\dot{\psi}_1 = -309.2rad/s$  and  $\dot{\psi}_2 = 6.061rad/s$ . For these cases, the graphs of  $U_{eff}$  are available in Fig. 5. It is seen that the minimum of  $U_{eff}$  is at  $\theta = 1.1rad$  and  $E'$  intersects  $U_{eff}$  at there.

In Eq. (38) we have three variables  $\theta$ ,  $\dot{\psi}$  and  $\dot{\phi}$ . We found  $\dot{\phi}$  by assigning values to others. It is also possible to find any one of the variables after assigning suitable values to others.

In this case, we can not use integration with respect to  $u$  to find the time, since only one  $u$  value is available. However we can integrate numerically angular accelerations, and results are available in Fig. 6. In Fig. 6, we see shapes of locus for regular precession with single  $\dot{\phi}$  and two  $\dot{\phi}$ . The first one is for the precession with single  $\dot{\phi}$ , seen at the left. Second and third one plotted on the same graph, seen at the right, since they precess without nutation at the same  $\theta$  value, they are overlapped and it looks like one line. One of them precessing in negative direction with greater angular velocity, the other one in the positive direction with smaller angular velocity. Results of  $\theta$ ,  $\phi$ ,  $\psi$ ,  $\dot{\theta}$ ,  $\dot{\phi}$  and  $\dot{\psi}$  (obtained from numerical integration of angular accelerations) for this and next cases are available in the appendix; Fig. 41 shows results for regular precession with single  $\dot{\phi}$ , Fig. 42 and Fig. 43 show results for regular

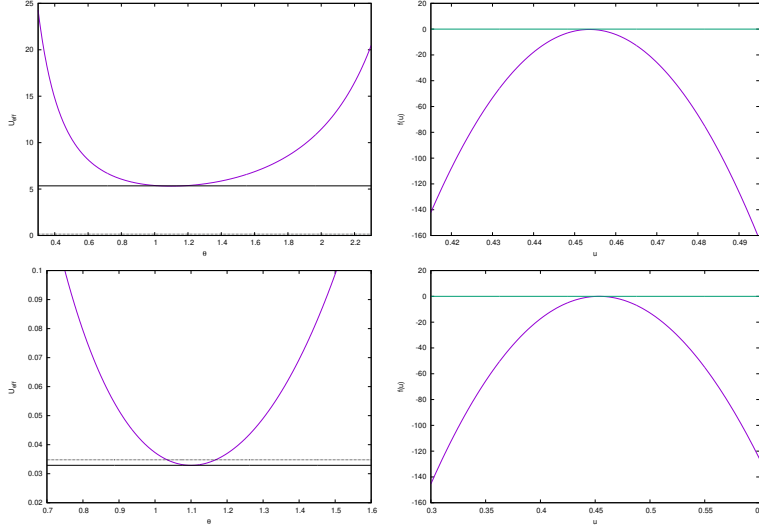


Figure 5: At left;  $U_{eff}$  and  $E'$  for  $\dot{\phi}_1$ (top  $E' = 5.346J$ ) and  $\dot{\phi}_2$ (bottom  $E' = 0.03289J$ ) for regular precession. At right; corresponding  $f(u)$ s. For the first one  $\dot{\psi}_0 = 50rad/s$ ,  $\theta_0 = 1.1rad$ ,  $\dot{\phi} = -309.2rad/s$ ,  $a = -141.8$ ,  $b = -309.9$ ,  $\alpha = 76370$  and  $Mglb/a = 0.1486$ . For the second one  $\dot{\psi}_0 = 50rad/s$ ,  $\theta_0 = 1.1rad$ ,  $\dot{\phi} = 6.061rad/s$ ,  $a = 82.89$ ,  $b = 42.41$ ,  $\alpha = 469.8$  and  $Mglb/a = 0.03479$ .

precession with two  $\dot{\phi}$ .

Here, it is better to mention some points. The gravitational force gives torque, if initial angular momentum is zero then this torque causes rotation around the line of nodes and  $\theta$  will increase. For the symmetric top, this torque is still available, however, for this regular precession case it does not result in an increase in  $\theta$ . This shows that there is an effect balancing this torque. If we look at the effective potential this effect is the result of  $I_x \dot{\phi}^2/2$ . This shows that for the symmetric top, the angular momentum around stationary  $z'$ -axis can cause a rise of the symmetric top. We will consider this rise with details in the next cases.

### 3.3 Cup like motion

For the cup like motion, it is better to start studying in terms of  $\dot{\psi}$ ,  $\dot{\phi}$ ,  $\dot{\theta}$  and  $\theta$ . This type of motion is one of the most seen cases.

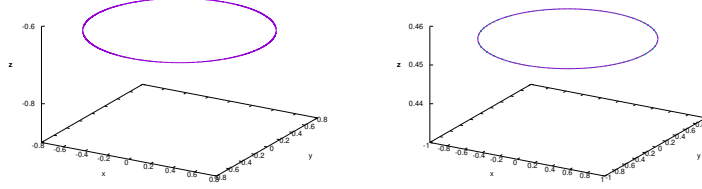


Figure 6: Shapes of the locus on unit sphere for the regular precession. The left one for the single  $\dot{\phi}$  with initial values  $\theta_0 = 2.269\text{rad}$ ,  $\phi_0 = 0$ ,  $\psi_0 = 0$ ,  $\dot{\theta}_0 = 0$ ,  $\dot{\phi}_0 = 36.36\text{rad/s}$ ,  $\dot{\psi}_0 = 17\text{rad/s}$ . (Animated version is available at <https://youtu.be/0ELpFh459CI> .) The right one for  $\dot{\phi}_1 = -309.2\text{rad/s}$  (continuous line) and  $\dot{\phi}_2 = 6.061\text{rad/s}$  (dashed line) with initial values  $\theta_0 = 1.1\text{rad}$ ,  $\phi_0 = 0$ ,  $\psi_0 = 0$ ,  $\dot{\theta}_0 = 0$ ,  $\dot{\psi}_0 = 50\text{rad/s}$ . (Animated version is available at <https://youtu.be/0fYYfVLhRVM> for backward precession and <https://youtu.be/xg0wpagyJyg> for forward precession.)

Now let us consider a symmetric top spinning with an initial angular velocity  $\dot{\psi}_0$ . If we let it spin with an initial inclination  $\theta_0$  and with zero angular velocities  $\dot{\phi}_0 = 0$  and  $\dot{\theta}_0 = 0$ , we see cup like motion.

Initially, the symmetric top will rotate an infinitesimal amount around the line of nodes by the effect of torque caused by the gravitational force and dependently  $\theta$  will increase. Then according to  $\dot{\phi} = (b - a \cos \theta) / \sin^2 \theta$ , the symmetric top will start to gain some angular velocity  $\dot{\phi}$ . As the magnitude of  $\dot{\phi}$  increases, the magnitude of  $\dot{\psi}$  will decrease according to the conserved quantity  $a$ .

We can see from the initial values that  $E' = Mgl \cos \theta_0$ , which is equal to the effective potential at that point. We also see from the initial values that  $b = a \cos \theta_0$  and if  $|b| < |a|$ , similar to this case, we can say  $\theta_0 = \arccos(b/a)$ , which makes  $E' = Mglb/a$ . Then one of the intersection angles of  $E'$  and  $U_{eff}$  occurs at  $\theta_0$ , which is the minimum since  $\theta$  increases after the start of the motion. As  $\theta$  increases  $U_{eff}$  decreases, this decrease is compensated by an increase in  $\dot{\theta}$  and the total energy remains constant. The increase in  $\theta$  gives the necessity of positive  $\dot{\theta}$ . From the shape of  $U_{eff}$ , we can conclude that after some time  $\theta$  will start to decrease and it will eventually be equal to 0 at the  $\theta_{max}$ . After  $\theta_{max}$ ,  $\dot{\theta}$  will have negative values and the symmetric

top will rise till  $\theta$  reaches its initial value.  $\dot{\theta}$  should be naturally zero at the turning angles and have extrema at  $\theta$  values where the minimum value of  $U_{eff}$  occurs.

In this case  $b = a \cos \theta_0$ , and if we consider  $\dot{\phi} = (b - a \cos \theta) / \sin^2 \theta$  relation we can understand the changes in  $\dot{\phi}$ . We have mentioned that  $\dot{\phi}$  will gain some angular velocity as  $\theta$  increases. During this motion, the magnitude of  $\dot{\phi}$  will reach the maximum value when  $\theta$  reaches its maximum value. After reaching the maximum value,  $\theta$  will gradually decrease and dependently  $\dot{\phi}$  will also decrease. When  $\theta$  returns to its initial value,  $\dot{\phi}$  will also and become zero. The magnitude of  $\dot{\psi}$  will firstly decrease and then increase to its initial value corresponding to changes in  $\dot{\phi}$ . All changes are similar to harmonic motion, but not exactly the same.

The turning angles of  $\theta$  are two important parameters of the motion. In this case, we have seen that  $\theta_0$  is the minimum angle. The maximum angle can be found from  $f(u)$  or from the solution of  $U_{eff} = E'$ .

For a case with initial values  $\theta_0 = 0.175rad$ ,  $\phi_0 = 0$ ,  $\dot{\theta}_0 = 0$  and  $\dot{\psi}_0 = 100rad/s$ , we obtained results. With these initial values constants in  $f(u)$  becomes  $a = 157.1$ ,  $b = 154.7$  and  $\alpha = 956.6$ . The results are depicted in Fig. 7, 8 and 9. At left of Fig. 7, we see the general structure of  $f(u)$ , and at right we see close view of it and the relevant roots,  $u_1 = 0.9834$  and  $u_2 = 0.9847$ . Corresponding  $\theta$  values to these roots are  $\theta_1 = 0.1823$  and  $\theta_2 = 0.1750rad$ .

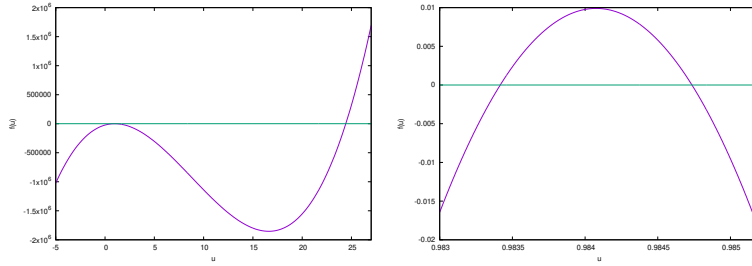


Figure 7:  $f(u)$  (left) and its close view (right) for  $a = 157.1$ ,  $b = 154.7$  and  $\alpha = 956.6$ . Roots occur at  $u = 0.9834$  and  $u = 0.9847$ .

In Fig. 8, we see  $U_{eff}$  and  $E'$  for this situation. From the graph we see possible  $\theta$  values; for physical cases,  $E'$  should be greater than  $U_{eff}$ , which is possible if  $\theta$  is between  $0.1750$  and  $0.1823rad$ . From this graph, we can say that the motion of the symmetric top in  $\theta$  will be periodic between these two turning angles. It starts from the initial  $\theta$  value,  $0.1750rad$ , then as a result



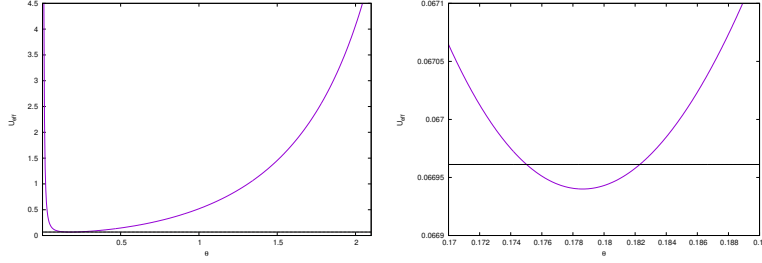


Figure 8:  $U_{eff}$  and  $E'$ , and its close view (right). It is seen that  $\theta$  can take values between  $0.1750$  and  $0.1823\text{rad}$  when  $E' = Mglb/a = 0.06696J$ . The minimum of  $U_{eff}$  ( $0.06694J$ ) is at  $0.1786\text{rad}$ . Initial values are  $\theta_0 = 0.175\text{rad}$ ,  $\dot{\theta}_0 = 0$ ,  $\dot{\phi}_0 = 0$  and  $\dot{\psi}_0 = 100\text{rad/s}$  and resulting constants are the same as Fig. 7.

of the gravitational force the symmetric top will fall and  $\theta$  will gradually increase till  $0.1823\text{rad}$ . Then, the symmetric top will return from that angle and continue its motion toward the other turning angle and the motion will continue in this way.

Using Eq. (33), we can find  $\theta(t)$  and  $\dot{\theta}(t)$ , and then using  $\theta(t)$  we can find  $\dot{\phi}(t)$  and  $\dot{\psi}(t)$  from Eqs (25) and (26). Due to the structure of Eq. (33), we need to consider one period in two parts; from  $\theta_{min}$  to  $\theta_{max}$  and then from  $\theta_{max}$  to  $\theta_{min}$ . In this procedure, there can be some discontinuities due to this separation. The results are shown in Fig. 9.

From  $U_{eff}$ , we made conclusions about  $\theta$  and  $\dot{\theta}$ . The mentioned changes for  $\theta$  and  $\dot{\theta}$  can be seen in Fig. 9. We also see changes in  $\dot{\phi}$  and  $\dot{\psi}$  at that figure. Now let us consider these changes in terms of conserved quantities, which show themselves as constants  $a$  and  $b$ .  $b$  corresponds to the conservation of angular momentum in  $z'$ , a component of  $\dot{\psi}$  contribute to it via  $a \cos \theta$ . As  $\theta$  increases this contribution decreases, then the conservation of the angular momentum in  $z'$  direction assures an increase in the magnitude of  $\dot{\phi}$ . But this increase should also be consistent with the conservation of the angular momentum in  $z$ -direction, related to  $a$ , and as the magnitude of  $\dot{\phi}$  increases, the magnitude of  $\dot{\psi}$  should decrease. After the maximum  $\theta$  value,  $\theta$  starts to decrease and the mentioned changes happen in the reverse order. We can see how these took place from the graphs in Fig. 9.

We see that  $\dot{\phi}$  is at the maximum when  $\theta$  is at the maximum, and zero when it is minimum, so the symmetric top precesses in a slower rate when

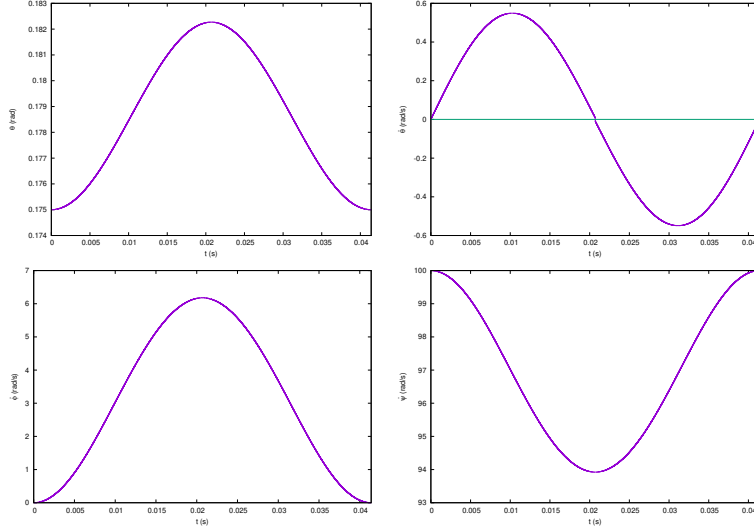


Figure 9:  $\theta(t)$  (up left),  $\dot{\theta}(t)$  (up right),  $\dot{\phi}(t)$  (down left) and  $\dot{\psi}(t)$  (down right), obtained by integration of Eq. (33). Initial values are the same as Fig. 8.

$\theta$  is near to its minimum. This produces a cup like figure if we draw a three-dimensional figure.

We have obtained changes in variables with respect to time by numerically integrating angular accelerations. The three-dimensional plots are available in Fig. 10. Plots for angles and angular velocities are available in the appendix, Fig. 44. All angular velocities oscillate due to torque felt by the symmetric top and obey conservation of angular momenta and energy;  $a$ ,  $b$  and  $E'$ .

In this type of motion,  $\dot{\phi}$  will have positive values if  $a$  is positive, and if  $a$  is negative it will have negative values. For the cup like motion,  $b$  can take values between  $-a$  to  $a$  depending on  $\theta_0$ .

Now, we can explain the rise of the symmetric top in terms of the angular momentum in  $z'$ -axis. In the previous case, we have seen that the gravitational torque is balanced by an effect caused by the angular momentum in  $z'$ -axis. The gravitational torque is parallel to the line of nodes. If we consider  $\vec{w} \times \vec{L}$  term, Eq. (4), and take the cross product of  $\vec{w}$  with the angular momentum in  $z'$  direction we obtain a vector anti-parallel to the line of nodes. This is also possible if the angular momentum is in  $-z'$  direc-

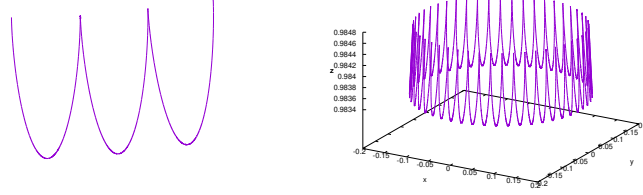


Figure 10: Shapes of the locus on unit sphere for the cup like motion. At the left we see a few nutation period, and at the right we see precession for  $2\pi$ . Initial values are the same as Fig. 8. ( Animated version is available at <https://youtu.be/UxhQCDL8YuQ> .)

tion. This vector acts like torque and it is available because of the symmetric top's being a non-inertial reference frame. It is just like the inertial forces or pseudo-forces appeared in non-inertial reference frames, and we will refer it by *inertial torque*.

In this case, at the beginning  $\dot{\phi}$  was zero and it was gradually increasing. Then, we can say that at the beginning, the magnitude of the gravitational torque was greater than the magnitude of the inertial torque. But after some time the magnitude of the inertial torque around the line of nodes becomes equal to the magnitude of the gravitational torque, at that moment  $\dot{\theta}$  reaches its maximum value and the minimum value of  $U_{eff}$  occurs. However,  $\theta$  continues to increase some more time. When  $\dot{\theta}$  reaches zero, the magnitude of the inertial torque around the line of nodes is already greater than the gravitational torque. This difference results with a negative torque around the line of nodes and negative  $\ddot{\theta}$ , as a result of this the symmetric top rises. As it rises the  $\dot{\phi}$  becomes smaller, and at a point again the torque around the line of nodes becomes zero, where again the minimum value of  $U_{eff}$  occurs. This rise continues for a while as a consequence of negative  $\ddot{\theta}$ . Finally,  $\theta$  reaches its initial value and rise stops, where  $\dot{\phi}$  is zero. Then this procedure repeats itself.

### 3.4 Wavy precession

In this case, we will consider that the symmetric top precesses toward the same direction at both  $\theta_{min}$  and  $\theta_{max}$ , and nutation takes place many times

during one precession. This kind of motion is possible if the initial  $\dot{\phi}$  is different than zero, and it should have the same sign at both extrema of  $\theta$ .

$\dot{\phi} = (b - a \cos \theta) / \sin^2 \theta$ , then it will be equal to the zero if  $\theta = \arccos(b/a)$ , which requires  $|b| < |a|$ . If we use  $\theta = \arccos(b/a)$  in  $U_{eff}$ , we obtain it as  $Mglb/a$ .  $E'$  determines possible interval of  $\theta$  according to  $U_{eff}$ , and if  $E'$  is smaller than  $Mglb/a$  then  $\theta$  does not take values which makes  $\dot{\phi}$  equal to zero. Since  $\dot{\phi}$  is a continuous quantity then  $\dot{\phi}$  does not change sign and always precesses in one direction in this case. Then we can say that to obtain this kind of motion the absolute value of  $b$  should be smaller than the absolute value of  $a$ , and  $E'$  should be smaller than  $Mglb/a$ , and  $Mglb/a$  should be greater than  $U_{eff}$ . In this case  $|b| > |a \cos \theta|$ .

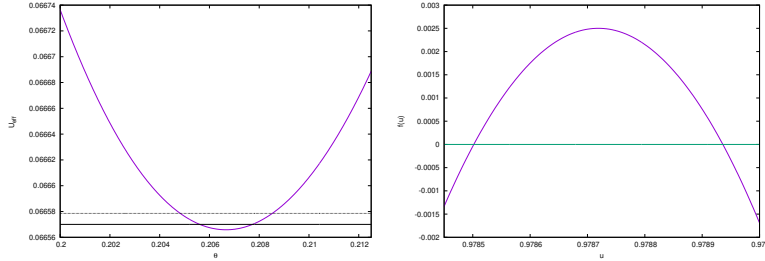


Figure 11:  $U_{eff}$ ,  $E'$  (black straight line),  $Mglb/a$  (dotted line) at left and  $f(u)$  at right. This case gives wavy precession, and initial values for this case as follows;  $\theta_0 = 0.2056rad$ ,  $\dot{\theta}_0 = 0$ ,  $\psi_0 = 148.3rad/s$ ,  $\dot{\phi} = 0.8968rad/s$  and resulting  $E' = 0.06657J$ . Turning angles for  $\theta$  are 0.2056 and 0.2077rad, and the minimum of  $U_{eff}$  is at 0.2067rad. For this case  $a = 234.4$ ,  $b = 229.5$  and  $\alpha = 951.0$ .

To obtain such a case we can choose  $\theta_0 = 0.2056rad$ ,  $\dot{\theta}_0 = 0$ ,  $\dot{\phi}_0 = 0.8968rad/s$  and  $\dot{\psi}_0 = 148.3rad/s$ . With these initial values, the constants become  $a = 234.4$ ,  $b = 229.5$  and  $\alpha = 951.0$ . Then,  $Mglb/a = 0.06658J$  and  $E' = 0.06657J$ , which is smaller than  $Mglb/a$ . The turning angles of  $\theta$  are 0.2056 and 0.2077rad, and these can be obtained from  $U_{eff}$  by using  $E'$  or from  $f(u)$ , whose plots are available in Fig. 11.

In Fig. 12, we see the results obtained numerically from Eq.s (33), (25) and (26). The initial value of  $\theta$  is the minimum value, then as time passes it increases in the first part of motion. We can understand this change from  $U_{eff}$ , as  $\theta$  increases  $\dot{\theta}$  increases till the minimum of the effective potential then starts to decrease. As  $\theta$  increases,  $\dot{\phi}$  increases to obey conservation

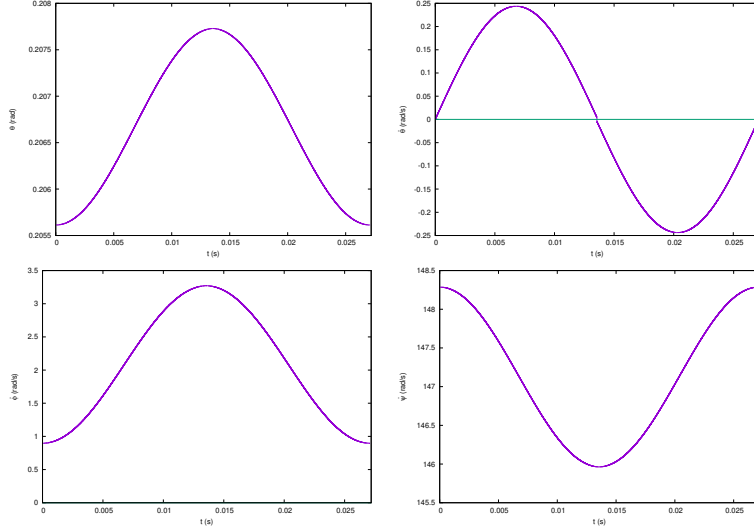


Figure 12:  $\theta$ (up left),  $\dot{\theta}$ (up right),  $\dot{\phi}$ (down left) and  $\dot{\psi}$ (down right) are obtained from the integration of Eq. (33). Initial values are the same as Fig. 11.

of angular momentum in  $z'$ -direction since  $a \cos \theta$  decreases, seen from  $b = \dot{\phi} \sin^2 \theta + a \cos \theta$ . As  $\dot{\phi}$  increases,  $\dot{\psi}$  decreases in accordance with conservation of angular momentum in  $z$ -direction, seen from  $a = (I_z/I_x)(\dot{\psi} + \dot{\phi} \cos \theta)$ . When  $\theta$  reaches its maximum,  $\dot{\theta}$  becomes zero. In the second half of the motion these changes take place in the reverse order.

By numerically integrating angular acceleration for the mentioned initial values we obtained results. Three-dimensional plots are available in Fig. 13, other results can be found in the appendix, Fig. 45. Wavy structure of the precession is visible in the three-dimensional figure.

This kind of motion can take place as long as the absolute value of  $b$  is smaller than the absolute value of  $a$ , i.e.  $|b| < |a|$ , provided that  $U_{eff_{min}} < E' < Mglb/a$ . If  $a$  is positive,  $\dot{\phi}$  becomes always positive and the symmetric top precesses always in the forward direction. If  $a$  is negative,  $\dot{\phi}$  becomes always negative and the symmetric top precesses in the backward direction.

If we consider the motion in terms of the gravitational torque and the angular momentum in  $z'$  direction, we can say that at the beginning of the motion the component of the inertial torque in the direction of the line of nodes, obtained from  $\vec{w} \times \vec{L}_{z'}$ , is smaller than the gravitational torque. Then

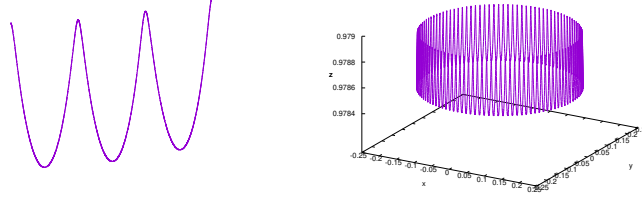


Figure 13: Shapes of the locus on unit sphere for the wavy precession. Initial values are the same as Fig. 11. ( Animated version is available at [https://youtu.be/rCs\\_XorW6mQ](https://youtu.be/rCs_XorW6mQ) .)

the symmetric top falls and  $\theta$  increases, meanwhile this increase resulted with an increase in  $\dot{\phi}$ . At some point, this increase resulted with a negative torque around the line of nodes. The consequences of this will not be seen immediately as a rise, this rise will be seen after it makes  $\dot{\theta}$  zero. Its effect is not enough to rise the symmetric top to reach the necessary height to provide negative  $\dot{\phi}$  values. After some time, the gravitational torque will become dominant and then the symmetric top will start to fall again. Then this motion will repeat itself.

### 3.5 Looping motion

If the symmetric top has both negative and positive  $\dot{\phi}$  and  $\dot{\theta}$  values, then the combination of motions forms a looping motion.

In this case,  $b - a \cos \theta$  should be equal to the zero for a value of  $\theta$  between  $\theta_{min}$  and  $\theta_{max}$ . Then  $\dot{\phi}$  becomes sometimes positive, sometimes negative and zero in between. Zero of  $\dot{\phi}$  occurs at  $\theta = \arccos(b/a)$ , this requires  $|b| < |a|$  because of the possible range of  $\cos \theta$ . We have seen in the previous case that if  $E' < Mglb/a$  then  $\dot{\phi}$  never becomes zero and always gets the same sign. So for the looping motion,  $E'$  should be bigger than  $Mglb/a$ . Then,  $\dot{\phi}$  will have a reverse sign for some  $\theta$  values and it will precesses toward different directions at  $\theta_{min}$  and  $\theta_{max}$ . So, the conditions for the looping motion can be written as  $\theta_{min} < \arccos(b/a) < \theta_{max}$  and  $E' > Mglb/a > U_{eff_{min}}$  provided that  $|b| < |a|$ . Since the symmetric top precesses in one direction at  $\theta_{min}$  and in other direction at  $\theta_{max}$ , there will be a looping motion.

Now, we will get results for this looping motion. We will choose the

initial values to provide that  $\dot{\phi}$  have negative and positive values at the extrema of  $\theta$ . To obtain such a case, we can choose  $\theta_0 = 0.27rad$ ,  $\dot{\theta}_0 = 0$ ,  $\dot{\phi}_0 = 10rad/s$  and  $\dot{\psi}_0 = 100rad/s$ . With these initial values, the constants become  $a = 172.3$ ,  $b = 166.8$  and  $\alpha = 943.3$ . In this case  $E' = 0.06603J$  and  $Mglb/a = 0.06582J$ . The turning angles of  $\theta$  are  $0.2472$  and  $0.2700rad$ , and these can be obtained from the effective potential by using  $E'$  or  $f(u)$ , their graphs are available in Fig. 14.

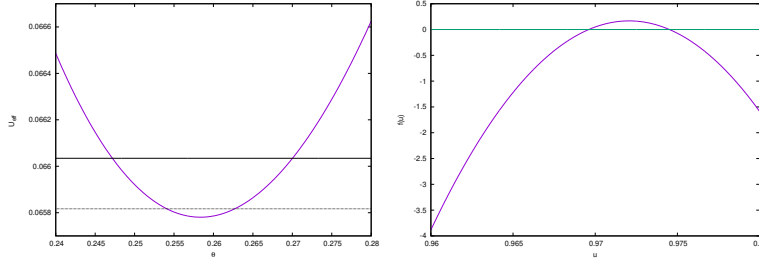


Figure 14:  $U_{eff}$ ,  $E'$  (black straight line) and  $Mglb/a$  (dotted line) at left, and  $f(u)$  at right. This case gives looping motion, and initial values for this case as follows;  $\theta_0 = 0.27rad$ ,  $\dot{\theta}_0 = 0$ ,  $\dot{\psi}_0 = 100rad/s$ ,  $\dot{\phi} = 10rad/s$  and resulting  $E' = 0.06603J$ . Turning angles for  $\theta$  are  $0.2472$  and  $0.27rad$ , and the minimum of  $U_{eff}$  is at  $0.2583rad$ . For this case  $a = 172.3$ ,  $b = 166.8$  and  $\alpha = 943.3$ .

Let us again start to analyze the motion from  $U_{eff}$ . This time the motion starts with the maximum  $\theta$  value since initial  $\dot{\phi}_0$  and  $a$  are positive, then the most of changes happen in reverse order with respect to previous cases. From the effective potential, we can conclude that  $\theta$  will reduce till the smaller turning angle,  $0.2472rad$ , and then increase till its initial value. Since the minimum of  $U_{eff}$  is at  $\theta = 0.2583rad$ , at these values  $\dot{\theta}$  should have extremum values.

Now let us analyze motion in terms of conservation of angular momenta. The results obtained by integration of Eq. (33) are seen in Fig. 15. We see that the motion is started from the maximum  $\theta$ , then it decreases as time passes. As it decreases, the contribution from constant  $a$  in  $b$  increases and  $\dot{\phi}$  should decrease to obey conservation of angular momentum in  $z'$ -direction, and this decrease continues to negative values. As  $\dot{\phi}$  decreases its contribution in  $a$  decreases, then  $\dot{\psi}$  should increase to obey conservation

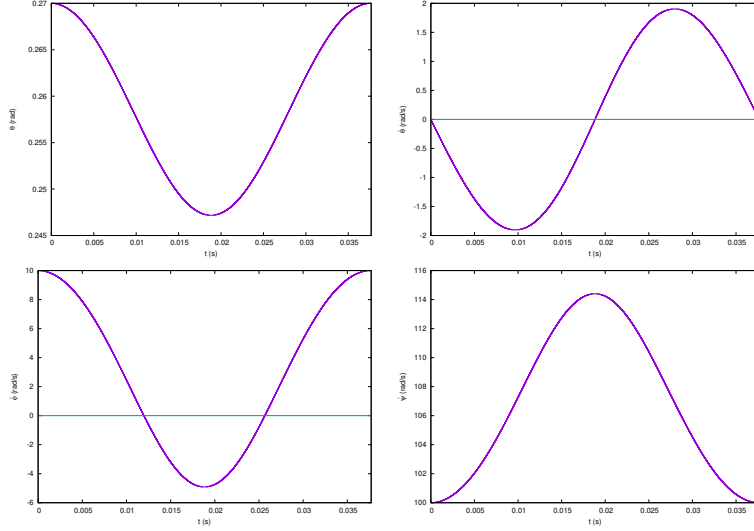


Figure 15:  $\theta$ (up left),  $\dot{\theta}$ (up right),  $\dot{\phi}$ (down left) and  $\dot{\psi}$ (down right) are obtained from the integration of Eq. (33). Initial values are the same as Fig. 14.

of angular momentum in  $z$ -direction. We also see that  $\dot{\phi}$  is positive at the maximum value of  $\theta$ , and it is negative at the minimum value of  $\theta$ .

The three-dimensional graphs obtained from numerical integration of angular accelerations are seen in Fig. 16. Looping structure is clearly seen. Other results are available in the appendix, Fig. 46.

If  $a$  is positive, then at the maximum of  $\theta$ ,  $\dot{\phi}$  is positive, and it is negative at the minimum. If  $a$  is negative,  $\dot{\phi}$  takes reverse signs.

Now let us consider the motion in terms of angular momentum and torque. This motion starts from  $\theta_{max}$  since  $\dot{\theta}_0 = 0$  and  $\dot{\phi}$  and  $a$  are positive. The inertial torque in the direction of the line of nodes originated from  $\dot{\phi}$  is big enough to rise the symmetric top to have negative  $\dot{\phi}$  values. At the negative  $\dot{\phi}$  values,  $\vec{w} \times \vec{L}_{z'}$  contribute to the gravitational torque in the same direction, then the symmetric top falls till reaching the initial  $\theta$  and  $\dot{\phi}$  value. The mentioned procedure repeats itself and the average value of  $\phi$  changes in every looping motion.



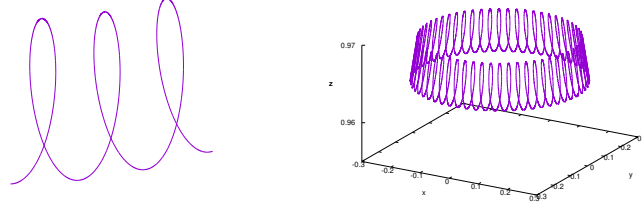


Figure 16: Shapes of the locus on unit sphere for looping motion. The initial values are the same as Fig. 14. ( Animated version is available at <https://youtu.be/hA3DCV7AbVc> .)

### 3.6 Precession with single nutation

In the cup like motion, the wavy precession and the looping motion, the absolute value of  $b$  was always smaller than the absolute value of  $a$ . Now we will consider that  $|b| > |a|$ . In the regular precession, there were some cases with  $|b| > |a|$ , however, at that cases there was no nutation. In the wavy precession,  $\dot{\phi}$  was having always the same sign with a careful determination of  $E'$ , with this determination possible  $\theta$  values was resulting with always the same sign for  $\dot{\phi}$  though  $|b| < |a|$  and there were many nutations in one precession. Differently from that case, in this case there will be nearly one nutation during one precession and  $\dot{\phi}$  will have always the same sign as a result of  $|b| > |a|$ .  $|b| > |a|$  provides precession always in the same direction independent of  $\theta$ , with  $E' > Mglb/a$  and  $E' > U_{effmin}$ .

In this one, we will choose initial values to provide that  $\dot{\phi}$  is always positive and different than zero with condition  $|b| > |a|$ . If we use initial values  $\theta_0 = 1.310rad$ ,  $\dot{\theta}_0 = 0$ ,  $\dot{\phi}_0 = 190rad/s$  and  $\dot{\psi}_0 = 100rad/s$ , then we obtain such a motion. With these initial values, the constants become  $a = 234.1$ ,  $b = 237.7$  and  $\alpha = 33950$ . By using  $f(u)$  or  $U_{eff}$  and  $E'$ , we find extrema of  $\theta$  as  $0.02013$  and  $1.310rad$  for this configuration.

Graphs of  $f(u)$  and  $U_{eff}$  are available in Fig. 17. If we look at the shape of  $U_{eff}$  from the graph, we see that it has a high asymmetry and the minimum value of  $U_{eff}$  is very close to the smaller turning angle. This asymmetry causes very rapid changes in  $\dot{\theta}$  near that turning angle.

By using integral in Eq. (33), we obtained  $\theta$ ,  $\dot{\theta}$ ,  $\phi$  and  $\psi$ , available in Fig. 18.  $\theta$  starts from the maximum value, then it gradually reduces, and as it

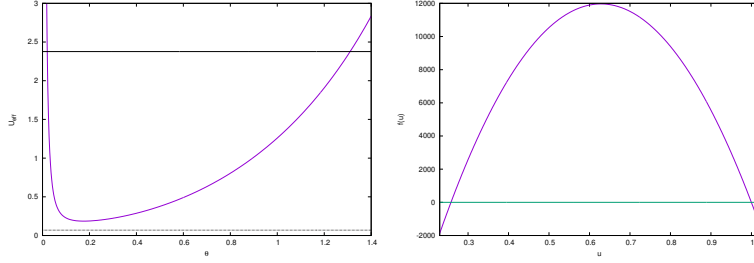


Figure 17:  $U_{eff}$ ,  $E'$  (straight black line),  $Mglb/a$  (dotted line) at left and  $f(u)$  at right. This case gives precession with single nutation, and initial values for this case as follows;  $\theta_0 = 1.310rad$ ,  $\dot{\theta}_0 = 0$ ,  $\dot{\psi}_0 = 100.0rad/s$ ,  $\dot{\phi} = 190rad/s$  and resulting  $E' = 2.377J$  and  $Mglb/a = 0.06905$ . Turning angles for  $\theta$  are  $0.02013$  and  $1.310rad$ , and the minimum of  $U_{eff}$  ( $0.186145$ ) is at  $0.1760rad$ . For this case  $a = 234.1$ ,  $b = 237.7$  and  $\alpha = 33950$ .

comes closer to the minimum value its change becomes more rapid. We see that  $\theta$  decreases till the minimum  $\theta$  value, then a sharp change occurs and  $\theta$  start to increase. This sharp change is seen in  $\dot{\theta}$  in a better way;  $\dot{\theta}$  reaches its minimum value, a negative one, then it starts to increase and becomes zero. After turning angle of  $\theta$ ,  $\dot{\theta}$  suddenly increases to its maximum value and then gradually decreases to zero.

The change in  $\dot{\phi}$  is more interesting, it starts with its positive initial value then decreases but do not reach zero. Before the symmetric top having its minimum  $\theta$  value, there is a sudden increase in  $\dot{\phi}$  and then it reaches to its maximum value, more than 40 times of its initial value, at the minimum of  $\theta$ . At the same time, there occurs a sudden change in  $\dot{\psi}$ , while it was decreasing gradually from its initial value it suddenly drops to very high negative values.

Now let us analyze these from conservation of angular momenta. If we consider constant  $b = \dot{\phi} \sin^2 \theta + a \cos \theta$ , as  $\theta$  decreases  $\cos \theta$  increases and  $\dot{\phi}$  should decrease to compensate this and preserve angular momentum  $z'$ -direction. At the beginning of motion we see this decrease. However, as  $\theta$  approaches to  $\theta_{min}$ , very close to zero, the multiplication factor of  $\dot{\phi}$  becomes very small. To compensate this,  $\dot{\phi}$  takes very great values.

We have another constant of motion  $a$ , corresponding conservation of angular momentum in  $z$  direction. At the beginning of the motion, there is slight decrease in  $\dot{\phi}$ . In this part, the increase rate of  $\cos \theta$  is greater than that decrease, and then  $\dot{\phi} \cos \theta$  increases. Then  $\dot{\psi}$  decreases to compensate for

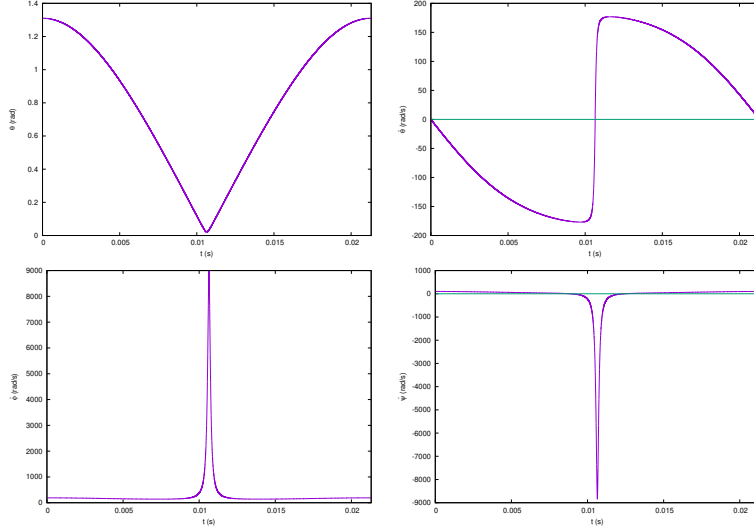


Figure 18:  $\theta$ (up left),  $\dot{\theta}$ (up right),  $\dot{\phi}$ (down left) and  $\dot{\psi}$ (down right) are obtained from the integration of Eq. (33). Initial values are the same as Fig. 17.

this increase. As motion continues,  $\dot{\phi}$  increases with an increasing rate. As  $\dot{\phi}$  becomes larger and larger,  $\dot{\psi}$  firstly becomes zero then takes high negative values to obey conservation of angular momentum.  $\dot{\psi}$  is related to the symmetric top's spin and its negative values mean that it spins in the reverse direction. The spin in the reverse direction is much faster than its initial value, more than 80 times. The symmetric top's spin in the reverse direction of its initial spin with very high values is a very interesting situation.

These changes happen during the rise of the symmetric top, after reaching turning angle the symmetric top starts to fall and all these changes happen in the reverse order.

There is another point related to this case; the symmetric top has nearly equal precession and nutation periods, nutation period is slightly greater than the precession period.

The three-dimensional graphs obtained from numerical integration of angular accelerations are available in Fig. 19. From the left one we see that nutation period and precession period is nearly the same, and from the right one we see that it slightly precesses forward after each nutation. Other results obtained from numerical integration of angular accelerations can be found in

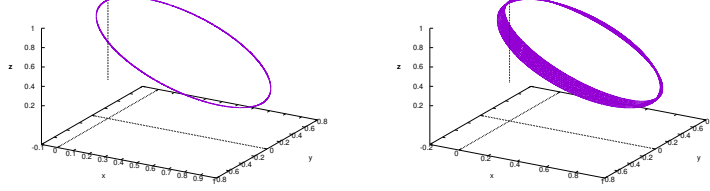


Figure 19: Shapes of the locus on unit sphere for precession with single nutation. Initial values are the same as Fig. 17. ( Animated version is available at <https://youtu.be/3g0gRb6CwaY> .)

the appendix, Fig. 47.

In this case, there are two possibilities; forward and backward precession. If  $b$  is positive, then the precession is forward and if  $b$  is negative it is backward, both cases are independent of the sign of  $a$ . This case is an example of the forward precession.

If we consider this case in terms of the torque and angular momentum, we can easily say that at the beginning the effect of  $\vec{w} \times \vec{L}_{z'}$  is bigger than the gravitational torque, and it rises the symmetric top. The rise continues up to very small  $\theta$  values. The astonishing changes in  $\dot{\phi}$  and  $\dot{\psi}$  are better understood from conservation of the angular momenta and we have already given the explanation. After the rise of the symmetric top to  $\theta_{min}$ ,  $\vec{w} \times \vec{L}_{z'}$  becomes very small because of very small  $\theta$  values and the gravitational torque becomes dominant and the symmetric top falls till  $\theta_0$ .

### 3.7 Precession with single nutation for weak top

In the previous case,  $E'$  was greater than  $Mglb/a$ . Now we will consider a case,  $|a| < |b|$  and  $U_{eff_{min}} < E' < Mglb/a$ . Previous case and this case are similar in many ways, however, for the completeness, we will analyze this case also. We should choose initial values according to these conditions, which require small  $|a|$  and  $|b|$  values. These small values can be obtained for weak top.

If we choose initial values as  $\theta_0 = 0.9225rad$ ,  $\dot{\theta}_0 = 0$ ,  $\dot{\psi}_0 = 1.225rad/s$  and  $\dot{\phi} = 22.21rad/s$  we obtain such a configuration. In this case constants of motion becomes  $a = 23$ ,  $b = 28$ ,  $\alpha = 900.0$ ; and we get  $E' = 0.06300J$  and

$$Mglb/a = 0.08278J.$$

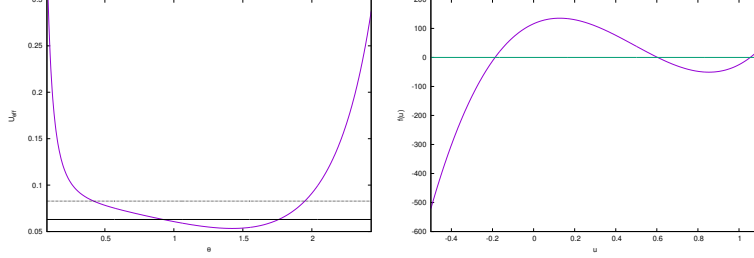


Figure 20:  $U_{eff}$ ,  $E'$  (straight black line) and  $Mglb/a$  (dotted line) at left, and  $f(u)$  at right. Initial values for this case as follows;  $\theta_0 = 0.9225rad$ ,  $\dot{\theta}_0 = 0$ ,  $\dot{\psi}_0 = 1.225rad/s$ ,  $\dot{\phi} = 22.21rad/s$  and resulting  $E' = 0.06300J$ . Turning angles for  $\theta$  are  $0.9225$  and  $1.759rad$ , and the minimum of  $U_{eff}$  is at  $1.423rad$  and equal to  $0.05336J$ . For this case  $a = 23$ ,  $b = 28$  and  $\alpha = 900.0$ .

In Fig. 20, we see  $U_{eff}$  and  $f(u)$ . It is also seen that  $E'$  is smaller than  $Mglb/a$ .  $E'$  and  $U_{eff}$  intersects when  $\theta$  is equal to  $0.9225$  and  $1.759rad$ . As it is seen, the smaller turning angle is away from  $\theta = 0$  point. This is related to the shape of  $U_{eff}$  and when  $a$  and  $b$  are small the minimum of the  $U_{eff}$  occurs at greater angles. Since initial  $\theta$  value is the minimum value, we can say  $\theta$  will increase till  $1.759rad$ .

Results obtained from the numerical integration of Eq. (33) are available in Fig. 21. It is seen that at the beginning  $\dot{\phi}$  slightly decreases as  $\theta$  increases. We can understand this decrease from conservation of angular momentum in  $z'$ -direction by using  $b = \dot{\phi} \sin^2 \theta + a \cos \theta$ ; the increase in  $\sin^2 \theta$  is faster at the beginning and to compensate it  $\dot{\phi}$  decreases. As  $\theta$  increases, the decrease in  $\cos \theta$  becomes dominant and  $\dot{\phi}$  increases to compensate it. We can understand the increase in  $\dot{\psi}$  from the mentioned decrease in  $\cos \theta$  from conservation of angular momentum by using  $a = (I_z/I_x)(\dot{\psi} + \dot{\phi} \cos \theta)$ ; its decrease is faster than the increase in  $\dot{\phi}$  in the second part and to compensate it  $\dot{\psi}$  increases. The increase in the first part can be understood from decrease of both  $\dot{\phi}$  and  $\cos \theta$ .

By integrating angular accelerations numerically, we plotted three-dimensional figure for this case, available in Fig. 22. We see that again nutation and precession periods are nearly equal, however, differently from the previous case nutation period is a bit smaller than precession period and interval for  $\theta$  does

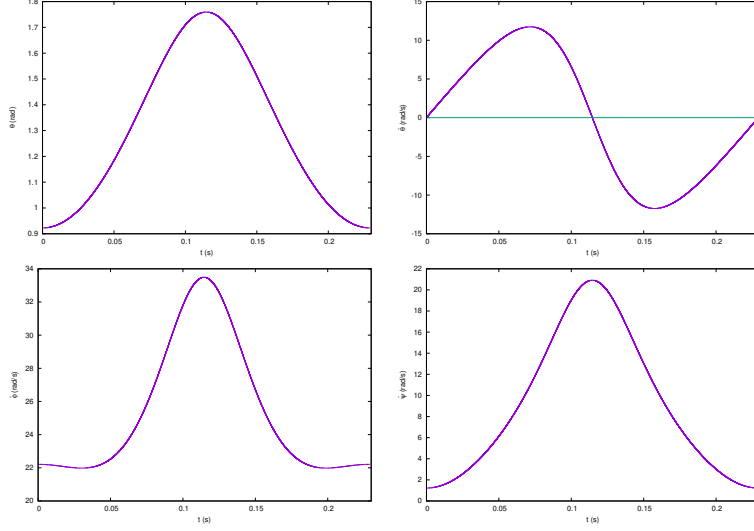


Figure 21:  $\theta$ (up left),  $\dot{\theta}$ (up right),  $\dot{\phi}$ (down left) and  $\dot{\psi}$ (down right) are obtained from the integration of Eq. (33). Initial values are the same as Fig. 20.

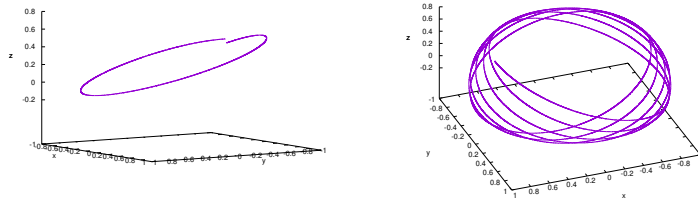


Figure 22: Shapes of the locus on unit sphere precession with single nutation for weak top. Initial values are the same as Fig. 20. ( Animated version is available at [https://youtu.be/\\_W\\_sTyeSNkI](https://youtu.be/_W_sTyeSNkI).)

not cover small values. Then the three-dimensional figure becomes different than the previous case. Other results obtained from numerical integration of angular accelerations are available in the appendix, Fig. 48.

In this case, precession direction depends on the sign of  $b$ , if it is positive (negative) then the precession direction is positive (negative). Both  $b$  and  $a$  should have the same sign to be able to get  $E' < Mglb/a$ .

The motion starts from its minimum  $\theta$  value, though initially  $\dot{\phi}$  is different than zero, the inertial torque is smaller than the gravitational torque. This difference causes fall of the symmetric top. As the symmetric top falls,  $\dot{\phi}$  becomes greater, and then inertial torque increases. At some point, inertial torque becomes greater than gravitational torque as a result of the increase in  $\dot{\phi}$ , and eventually, it rises the symmetric top. Then this motion repeats itself.

### 3.8 Motion with the same precessional angular velocity at extrema

In one of the previous cases, we obtained the cup like motion when initial values satisfy  $E' = Mglb/a$  and  $b < a$ . In previous two cases for  $|b| > |a|$ ,  $E'$  was either greater or smaller than  $Mglb/a$ . In this case, we choose initial values to provide  $b > a$  and  $E' = Mglb/a > U_{eff_{min}}$ , and at the end, we get a really interesting result;  $\dot{\phi}$  becomes equal at  $\theta_{min}$  and  $\theta_{max}$ .

Let us rewrite Eq. (23') for  $E' = Mglb/a$ ; if we consider extrema of  $\theta$ , where  $\dot{\theta}$  becomes zero, then Eq. (23') becomes

$$Mgl \frac{b}{a} = \frac{I_x (b - a \cos \theta_{ext})^2}{2 \sin^2 \theta_{ext}} + Mgl \cos \theta_{ext}. \quad (42)$$

By taking  $Mgl \cos \theta_{ext}$  to the left-hand side and dividing both sides to  $b - a \cos \theta_{ext}$ , after some arrangement we get

$$\frac{b - a \cos \theta_{ext}}{\sin^2 \theta_{ext}} = \frac{2Mgl}{I_x a}. \quad (43)$$

Here the left-hand side is equal to  $\dot{\phi}$  when  $\theta = \theta_{ext}$ , then  $\dot{\phi}$  becomes  $2Mgl/(I_x a)$  at both extrema of  $\theta$ .

Now let us see this interesting case from an example. If we choose  $\theta_0 = 0.04097 \text{ rad}$ ,  $\dot{\theta} = 0$ ,  $\dot{\phi} = 41.51 \text{ rad/s}$  and  $\dot{\psi} = -26.59 \text{ rad/s}$ , we obtain;  $a =$

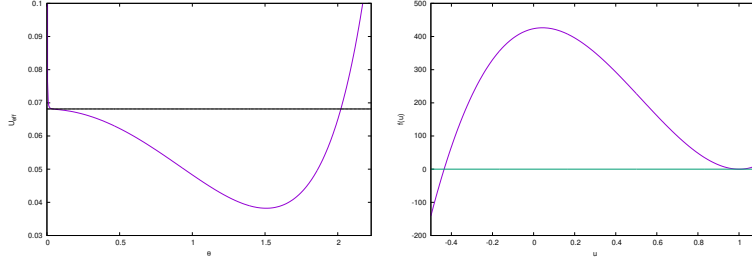


Figure 23:  $U_{eff}$  and  $E'$  at left,  $f(u)$  at right. This case gives motion with the same precessional angular velocity at extrema, and initial values for this case as follows;  $\theta_0 = 0.04097rad$ ,  $\dot{\theta}_0 = 0$ ,  $\dot{\psi}_0 = -26.59rad/s$ ,  $\dot{\phi} = 41.51rad/s$  and resulting  $E' = 0.06815J$ . Turning angles for  $\theta$  are  $0.04097$  and  $2.021rad$ , and the minimum of  $U_{eff}$  is at  $1.508rad$  and equal to  $0.03822J$ . The constants of motion:  $a = 23.4$ ,  $b = 23.45$  and  $\alpha = 973.5$ .

$23.4$ ,  $b = 23.45$  and  $E' = Mglb/a = 0.06815J$ . For this case turning angles becomes  $\theta_{min} = 0.04097$  and  $\theta_{max} = 2.021rad$ .

In Fig. 23, we see  $U_{eff}$  and  $f(u)$ . It is seen that  $\theta$  covers from very small values to values greater than  $\pi/2$ . By using our previous experience, we can say from  $U_{eff}$  and  $E'$  that the symmetric top will make a periodic motion between its two turning angles.

In Fig. 24, we see results obtained by numerical integration of Eq. (33). The results related to  $\theta$  and  $\dot{\theta}$  are compatible with  $U_{eff}$ . Asymmetry seen in  $\dot{\theta}$  near greater turning angle is a result of asymmetry in  $U_{eff}$ . We can understand changes in  $\dot{\phi}$  from conservation of angular momentum in  $z'$ -direction by using  $b$ . We see at the beginning  $\dot{\phi}$  decreases, this decrease compensates the increase in  $\sin \theta$  to preserve  $b$ . Then we see an increase in  $\dot{\phi}$ , this increase occurs to compensate the decrease in  $\cos \theta$  again to preserve  $b$ . When  $\theta$  becomes larger than  $\pi/2$ , both  $\sin \theta$  and  $\cos \theta$  decrease, and the increase in  $\dot{\phi}$  becomes more rapid. This increase continues till  $\dot{\phi}$  reaching its initial value, which is the result of choosing  $E' = Mglb/a$ .

Changes in  $\dot{\psi}$  can be explained from conservation of angular momentum in  $z$ -direction by using  $a$ . As  $\dot{\phi}$  decreases,  $\dot{\psi}$  increases to preserve  $a$ . When  $\dot{\phi}$  starts to increase the decrease rate of  $\cos \theta$  is faster and  $\dot{\psi}$  should still increase to preserve  $a$ . When  $\theta$  passes  $\pi/2$ , the contribution in  $a$  from  $\dot{\phi}$  becomes negative and the increase in  $\dot{\psi}$  becomes more rapid to obey conservation of angular momentum in  $z$ -direction.



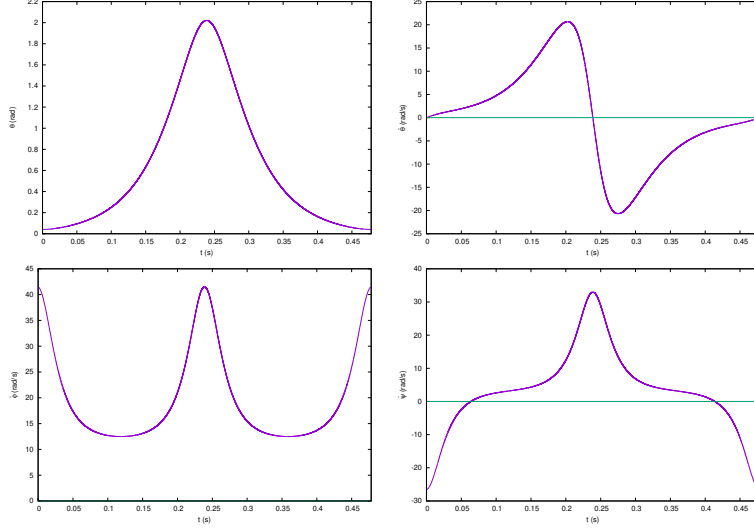


Figure 24:  $\theta$ (up left),  $\dot{\theta}$ (up right),  $\dot{\phi}$ (down left) and  $\dot{\psi}$ (down right) are obtained from the integration of Eq. (33). Initial values are the same as Fig. 23.

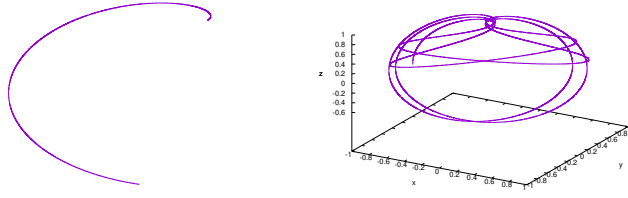


Figure 25: Shapes of the locus on unit sphere for motion with the same precessional angular velocity at extrema. Initial values are the same as Fig. 23. ( Animated version is available at <https://youtu.be/qLof6AgLRUY> .)

We see three-dimensional figures in Fig. 25. We see that the symmetric top makes a motion like a spiral without the inner part. We know that from the above calculations at the bottom and top  $\dot{\phi}$  has the same values, though the linear speeds at these points are different. Other results are available in the appendix, Fig. 49.

If we consider the motion in terms of torque and angular momentum, there is an interesting situation; we have the same  $\dot{\phi}$  at the bottom and top, however, in one case the symmetric top rises, in the other it falls. It is directly related to the cross product and existence of  $\sin \theta$ , which results with greater inertial torque with respect to gravitational torque at the bottom and results with smaller inertial torque at the top. Then when the symmetric top is at the bottom it rises gradually till reaching smaller turning angle, and when it is at the top it gradually falls. This structure repeats itself in the motion.

### 3.9 Motion through pseudo-singular points

We have seen that the effective potential has infinities at  $\theta = 0$  and  $\theta = \pi$ . These infinities occur because  $\sin \theta$  equals to zero at these angles. However, if we consider  $|b| = |a|$ , one of the singularities at these angles can be removed by simplifications. Now, we will study this interesting case.

In the sleeping top case, we have already dealt with  $|b| = |a|$  situation, however, in that case,  $b$  was becoming equal to  $\pm a$  because of overlapping.  $b$  corresponds to angular momentum in  $z'$ -direction and  $a$  corresponds to angular momentum in  $z$ -direction, then the equivalence of magnitudes of angular momenta assures equivalence of  $a$  and  $b$ , i.e. if  $L_z = \pm L_{z'}$  then  $b = \pm a$ . This time we will analyze the motion with  $b = a$  and without such an overlap.

If we choose  $\theta_0 = 1.2rad$ ,  $\dot{\theta}_0 = 0$ ,  $\dot{\phi}_0 = 198.2rad/s$  and  $\dot{\psi}_0 = 100rad/s$ , then  $b$  becomes equal to  $a$ ,  $b = a = 270.0$ . For this case  $f(u)$  is shown in Fig. 26. The roots of  $f(u)$  are  $u = 0.3624$  and  $1$ , which correspond  $1.2rad$  and  $0$  values for  $\theta$ . In this case, there is a difference between  $f(u)$  and  $U_{eff}$ , related to transformation,  $u = \cos \theta$ .

This case is different than all previously considered cases because of the disappearing infinity in  $U_{eff}$ , which is at  $\theta = 0$  for  $b = a$ . Then it is better to consider the previous restrictions on the motion. While considering Euler angles it is mentioned that usually the domain of  $\theta$  is considered as  $[0, \pi]$ . However, if we use this interval for  $\theta$ ,  $U_{eff}$  goes to its minimum at  $\theta = 0$  and leaves no turning angle in one side for the symmetric top. Now let us change

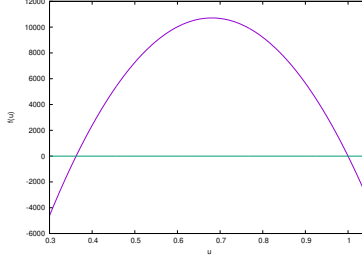


Figure 26:  $f(u)$ . This case is possible with initial values  $\theta_0 = 1.2rad$ ,  $\dot{\theta}_0 = 0$ ,  $\dot{\phi}_0 = 198.2rad/s$  and  $\dot{\psi}_0 = 100rad/s$ . Here  $E' = 2.413J$ . The roots of  $f(u)$  occur at  $u = 0.3624$  and  $1$  corresponding to turning angles for  $\theta$   $1.2rad$  and  $0$ . For this case constants:  $b = a = 270.0$  and  $\alpha = 34470$ .

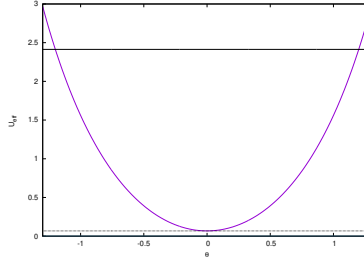


Figure 27:  $U_{eff}$ ,  $E'$  (straight black line) and  $Mglb/a$  (dotted line). Turning angles for  $\theta$  are  $1.2$  and  $-1.2rad$ , and the minimum of  $U_{eff}$  is at  $\theta = 0$  and equal to  $Mgl$ . Initial values and constants are the same as Fig. 26.

the interval of the domain to  $[-\pi, \pi]$ , and leave the evaluation of this change to the later. In Fig. 27, we see  $U_{eff}$  plotted for mentioned initial values with the extended domain. It is seen that the extended interval provides an effective potential with two turning angles.

When  $a = b$ , there are some simplifications and the effective potential becomes

$$U_{eff}(\theta) = \frac{I_x a^2 (1 - \cos \theta)}{2 (1 + \cos \theta)} + Mgl \cos \theta. \quad (44)$$

This difference in the effective potential brings the necessity of studying this case separately from previously studied types of moton.

In Fig. 28, we see the results obtained from the integration of Eq. (33).

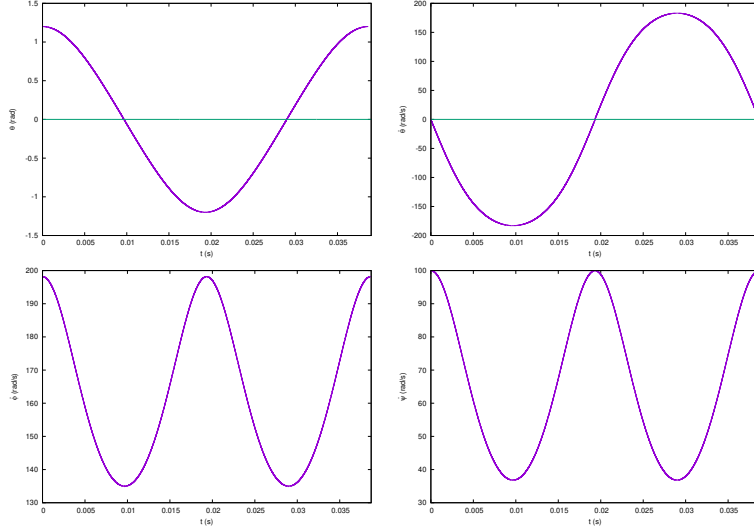


Figure 28:  $\theta$ (up left),  $\dot{\theta}$ (up right),  $\dot{\phi}$ (down left) and  $\dot{\psi}$ (down right) are obtained from the integration of Eq. (33). Initial values are the same as Fig. 26.

It is seen that the first half of the motion starts from  $\theta_{max} = 1.2rad$  and goes to  $\theta_{min} = -1.2rad$ , which is consistent with the effective potential. If we look at  $\dot{\theta}$ , it decreases to its minimum at  $\theta = 0$ . This shows that for this case the symmetric top approaches to  $\theta = 0$  with a negative angular velocity and it should continue its motion with that angular velocity. If we had kept the domain for  $\theta$  between 0 and  $\pi$ , then we need to change  $\dot{\theta}$  from negative to positive values. Since  $\dot{\theta}$  is a continuous quantity, it is better to change the domain of  $\theta$  to  $[-\pi, \pi]$  with keeping in mind that we are not using one to one mapping between coordinate systems.

If we return to the consideration of  $f(u)$ ; it does not give turning angle  $\theta = -1.2rad$ , it gives 0 and  $1.2rad$ . Trigonometric property of  $\cos \theta$  is lost during the change of variable, and we can not get results corresponding to the extended domain. In this work, in necessary cases we will use the extended domain to analyze the motion. In this case  $(\theta, \phi)$  and  $(-\theta, \phi + \pi)$  corresponds to the same points in  $xyz$  coordinate system. For this work it does not cause any trouble; three-dimensional plots will represent the motion without any problem.

If we look at the changes in  $\dot{\phi}$  and  $\dot{\psi}$ , there is a repeat. This is an

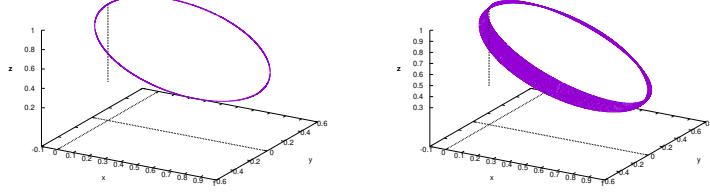


Figure 29: Shapes of the locus on unit sphere for motion through pseudo-singular points. Initial values are the same as Fig. 26. ( Animated version is available at <https://youtu.be/yHX8faDair4>.)

expected result since these two angular velocities are independent of  $\dot{\theta}$ , and  $\cos \theta$  is even and  $\sin \theta$  shows itself as a square in related equations. Here we can write  $\dot{\phi} = a/(1 + \cos \theta)$ , then as  $\theta$  goes to zero  $\dot{\phi}$  decreases. We can also understand this decrease from conservation of angular momentum by using  $b = \dot{\phi} \sin^2 \theta + a \cos \theta$ , as  $\theta$  goes to 0  $\cos \theta$  increases and  $\dot{\phi}$  decreases to obey conservation of angular momentum in  $z'$ -direction. As  $\dot{\phi}$  decreases  $\dot{\psi}$  is decreasing. The increase of  $\cos \theta$  is faster than the decrease in  $\dot{\phi}$  then  $\dot{\psi}$  also decreases to obey the conservation of angular momentum in  $z$ -direction, which can be seen from  $a = (I_z/I_x)(\dot{\psi} + \dot{\phi} \cos \theta)$ .

Here it is better to mention about one more point. In the sleeping top case, we claimed that  $\dot{\phi}$  becomes irrelevant from the motion. At there, it is irrelevant because  $z$  and  $z'$  are always the same. In this case,  $z$  and  $z'$  momentarily become equal and there is a motion which brings conservation of angular momentum. Then,  $\dot{\phi}$  should have some value at  $\theta = 0$ , which can be found from  $\dot{\phi} = a/(1 + \cos \theta)$  as  $a/2$ , and in this example we have  $\dot{\phi} = a/2 = 135 \text{ rad/s}$ .

Three-dimensional figures obtained from numerical integration of angular accelerations are available in Fig. 29. During numerical integration for very small values of  $\theta$  because of the singularity at  $\theta = 0$ , here and other necessary cases we have used Eq. (25) and Eq. (26). The apex of the symmetric top passes from  $\theta = 0$  and makes nearly a loop, however, there is a slight difference between periods of nutation and precession and the symmetric top precesses slightly at each loop like motion. Other results can be found in the appendix, Fig. 50.

In this case, the symmetric top precesses in the forward direction. If both  $a$  and  $b$  were negative, then the motion would be similar to this case but the symmetric top would precess backward. If  $b = -a$ , then the infinity of  $U_{eff}$  at  $\theta = \pi$  will disappear and the motion will take place at the bottom including  $\theta = -\pi$  point.

In this case, the positive  $\dot{\phi}$  causes an inertial torque to rise up the symmetric top, then it rises and passes from  $\theta = 0$  point. Then, the symmetric top falls from the other side of  $\theta = 0$  point and falls till  $-\theta_{max}$ , where it has its initial angular velocity  $\dot{\phi}$ . Then the motion repeats itself.

In the previous cases, the structure of the effective potential and the conservation of angular momenta were preventing the symmetric top to pass from  $\theta = 0$  point. However, in this case, the symmetric top passes from  $\theta = 0$  point since  $a = b$ .

### 3.10 Regular precession when $a = b$

There are other changes in the motion of the symmetric top when  $b = a$ . There are two main reasons for these; change in  $U_{eff}$  and  $\dot{\phi}$ . We already gave the effective potential when  $a = b$  as

$$U_{eff}(\theta) = \frac{I_x a^2 (1 - \cos \theta)}{2 (1 + \cos \theta)} + Mgl \cos \theta. \quad (44)$$

Here, if  $a$  is smaller than  $\sqrt{4Mgl/I_x}$  then there exist a local maximum at  $\theta = 0$ , which is equal to  $Mglb/a$  (or  $Mgl$ ). If  $a$  is greater than  $\sqrt{4Mgl/I_x}$ , this maximum becomes the minimum with the same value, the previous case, which is the motion through pseudo-singular points, is an example for such potential with minimum  $Mglb/a$ .

If a local maximum exists and  $E'$  is smaller than  $Mglb/a$  then we can obtain regular precession and two turning angles for  $\theta$  between 0 and  $\pi$ .

The other change is related to  $\dot{\phi}$ . When  $b = a$ ,  $\dot{\phi}$  becomes

$$\dot{\phi} = \frac{a}{1 + \cos \theta}. \quad (45)$$

Here,  $\dot{\phi}$  does not change sign and never become zero. Then we can not obtain cup like motion or looping motion.

Now we can consider the regular precession when  $a = b$ . In the previous study of the regular precession, the potential and  $\dot{\phi}$  were different than in

this case. In this case, if we take the derivative of  $U_{eff}$  with respect to  $\theta$  and equate it to zero we obtain

$$0 = \left[ \frac{I_x}{2} \frac{2a^2}{(1 + \cos \theta)^2} - Mgl \right] \sin \theta. \quad (46)$$

This time  $\theta = 0$  corresponds to unstable equilibrium or sleeping top and  $\theta = \pi$  corresponds to the sleeping top. Here, it is possible to find a minimum for the potential other than  $\theta = 0$  if  $a < \sqrt{4Mgl/I_x}$ . If  $a > \sqrt{4Mgl/I_x}$  the minimum of the effective potential occurs always at  $\theta = 0$ .

Here, it is also seen that previous strong and weak top definition in terms of  $\tilde{a}$  are consistent with  $b = a$  case.

By using Eq. (45) and Eq. (46), for regular precession  $\dot{\phi}^2$  is obtained as

$$\dot{\phi}^2 = \frac{Mgl}{I_x}. \quad (47)$$

This gives constant  $\dot{\phi}$  for regular precession, when  $a < \sqrt{4Mgl/I_x}$ .  $\dot{\phi}$  can have positive and negative values, positive (negative) one corresponds to positive (negative)  $a$ . By using the definition of  $a$  and Eq. (45), we obtain  $\dot{\psi}$  as

$$\dot{\psi} = \frac{I_x}{I_z} \dot{\phi} \left( 1 + \cos \theta - \frac{I_z}{I_x} \cos \theta \right). \quad (48)$$

Then we need to specify either  $\theta_0$  or  $\dot{\psi}_0$  and determine the other one from Eq. (48) to obtain a regular precession as long as there exists a local maximum. This case is simpler than  $b \neq a$  case and we can obtain the minimum of the  $U_{eff}$  in terms of constants in a simple way as

$$U_{eff_{min}} = \frac{\sqrt{I_x a^2}}{2} - (\sqrt{Mgl} - \sqrt{I_x a^2})^2. \quad (49)$$

For the symmetric top, that we are considering in this work,  $\dot{\phi}$  becomes  $22.04 \text{ rad/s}$  for the precession in the positive direction. If we choose  $\theta = 1.1 \text{ rad}$ , then  $\dot{\psi}$  becomes  $10.39 \text{ rad/s}$ . In this case  $b = a = 32.04$  and  $E' = U_{eff_{min}} = 0.05785$  together with  $\dot{\theta} = 0$ . In Fig. 30, we see  $U_{eff}$  and  $f(u)$ .  $E'$  intersects  $U_{eff}$  at its minimum and the symmetric top regularly precesses around  $z'$ -axis.

In Fig. 31, we see results obtained by numerical integration of angular acceleration. The symmetric top precesses in the positive direction. The other results are available in Fig. 51.

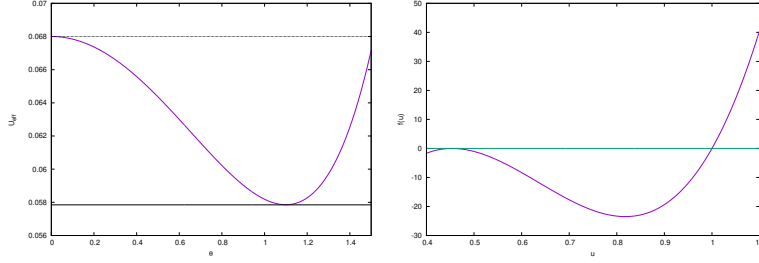


Figure 30:  $U_{eff}$ ,  $E'$  (straight black line)  $Mglb/a$  (dotted line) and left,  $f(u)$  at right. This case gives regular precession, and initial values for this case as follows;  $\theta_0 = 1.1rad$ ,  $\dot{\theta}_0 = 0$ ,  $\dot{\psi}_0 = 10.39rad/s$ ,  $\dot{\phi} = 22.04rad/s$  and resulting  $E' = 0.05785J$ . For this case:  $b = a = 32.04$  and  $\alpha = 826.4$ .

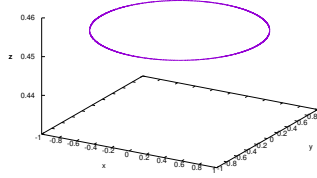


Figure 31: Shapes of the locus on unit sphere for regular precession when  $b = a$ . Initial values are the same as the ones given in Fig. 30. ( Animated version is available at <https://youtu.be/fNwjZQc08IY> .)

If we had chosen  $\dot{\phi}$  as  $-22.04rad/s$ , for  $\theta = 1.1rad$   $\dot{\psi}$  would be equal to  $-10.39rad/s$ , and the symmetric top would be precessing in the negative direction. With these negative values,  $a$  would be negative.

We have mentioned that if  $b = -a$ , then the singularity at  $\theta = \pi$  disappears, however, regular precession is not possible since there is no local maximum at  $\theta = \pi$ .

### 3.11 Precession in one direction when $a = b$

If there is a local maximum and  $E'$  is greater than  $U_{eff_{min}}$  and smaller than that local maximum, which is equal to  $Mglb/a$ , then we can obtain two



turning angles for  $\theta$  between 0 and  $\pi$ . We have seen that  $\dot{\phi}$  does not change sign when  $b = a$ . Then, in this case, we see only a precession in one direction and the direction of the precession is determined by the sign of  $a$ . Since  $\dot{\psi}$  is small for these configurations, the precession is faster and we do not see many nutations for one precession period.

If we take  $\theta_0 = 1.097\text{rad}$ ,  $\dot{\phi}_0 = 20.88\text{rad/s}$  and  $\dot{\psi}_0 = 9.824\text{rad/s}$ , then  $b = a = 30.4$ . In our example  $Mgl = 0.068J$ . Then together with  $\dot{\theta}_0 = 0$ ,  $E'$  becomes  $0.05518J$  which is smaller than  $Mglb/a$ . As it is expected from the sign of  $a$ , the precession is in the positive direction. We see  $U_{eff}$  and  $f(u)$  in Fig. 32 with these initial values. We see the possible interval for  $\theta$  from the figure. From the effective potential and  $E'$ , we can say that the symmetric top will nutate between two turning angles.

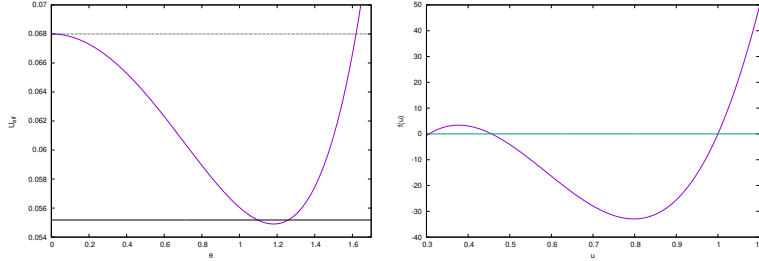


Figure 32:  $U_{eff}$ ,  $E'$  (straight black line),  $Mglb/a$  (dotted line) at left, and  $f(u)$  at right right. This case gives a precession in one direction and initial values for this case as follows;  $\theta_0 = 1.097\text{rad}$ ,  $\dot{\theta}_0 = 0$ ,  $\dot{\psi}_0 = 9.824\text{rad/s}$ ,  $\dot{\phi} = 20.88\text{rad/s}$  and resulting  $E' = 0.05518J$ . Turning angles for  $\theta$  are 1.097 and 1.259rad, and the minimum of  $U_{eff}$  is at 1.182rad. For this case:  $b = a = 30.40$  and  $\alpha = 788.3$ .

In Fig. 33, we see changes in  $\theta$  and angular velocities obtained by using Eq. (33). We see from the figure that  $\theta$  changes between two turning angles,  $\dot{\theta}$  have positive and negative values satisfying nutation.  $\dot{\phi}$  takes only positive values as we expected, and  $\dot{\psi}$  changes as  $\dot{\phi}$  changes obeying the conservation of angular momenta which can be seen from  $a$  and  $b$ . As  $\theta$  increases  $\dot{\phi}$  increases to obey conservation of angular momentum because of the decrease in  $\cos \theta$ , which can be understood by using  $b = \dot{\phi} \sin^2 \theta + a \cos \theta$ .  $\dot{\psi}$  increases again because of the decrease in  $\cos \theta$ , which can be understood from  $a = (I_z/I_x)(\dot{\psi} + \dot{\phi} \cos \theta)$ . Here we should mention that values of  $b$  and  $a$  are the same, but this case is different than sleeping top;  $b$  and  $a$  correspond different

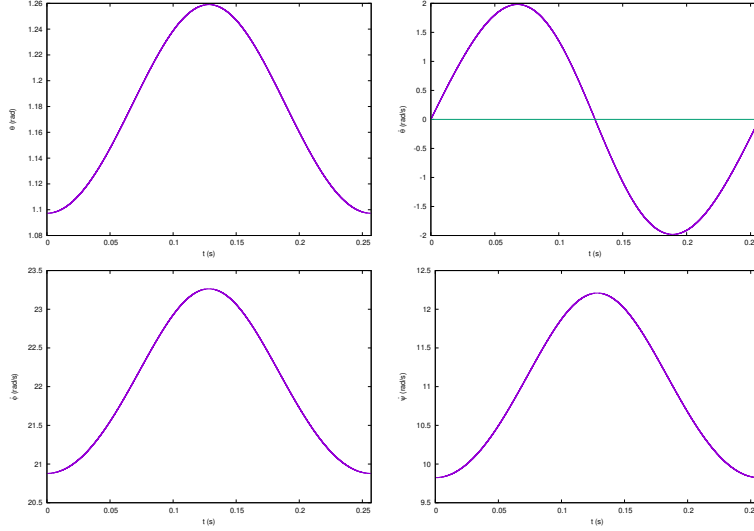


Figure 33:  $\theta$ (up left),  $\dot{\theta}$ (up right),  $\dot{\phi}$ (down left) and  $\dot{\psi}$ (down right) are obtained from the integration of Eq. (33). Initial values are the same as Fig. 32.

angular momenta and both are conserved separately. If we consider fall of the symmetric top, the initial  $\dot{\phi}$  is not enough to satisfy necessary torque and the gravitational torque is dominant. As the fall continues  $\dot{\phi}$  becomes great enough to cause a torque greater than gravitational one and the symmetric top rises. These repeat again and again as precession continues.

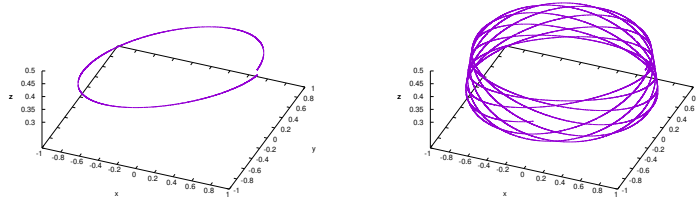


Figure 34: Shapes of the locus on unit sphere for precession in one direction when  $b = a$ . Initial values are the same as Fig. 32. ( Animated version is available at <https://youtu.be/PqJ8ubaiFTk>.)

In Fig. 34, we see three-dimensional figure obtained from the numerical integration of angular accelerations. It is seen that it precesses away from the  $\theta = 0$  point. The other results are available in the appendix, Fig. 52.

### 3.12 Spiraling motion

Now we will consider that  $E'$  is equal to the local maximum of  $U_{eff}$  at  $\theta = 0$  when  $b = a$ , we see graph of the effective potential for such a case in Fig. 35. From  $U_{eff}$ , it is seen that the turning angles occur at negative and positive  $\theta$  values and it is better to extend the domain of  $\theta$  with remembering that it corresponds double defined points in  $xyz$  coordinate system. If we do not use the extended domain while solving this case, there can be a problem at  $\theta = 0$  point about which direction the symmetric top will go at that point. When we use the extended domain, it continues its motion obeying conservation of angular momenta, so it is better to use the extended domain. We can say that the symmetric top will oscillate between these two turning angles while precessing. The existence of precession result with a spiraling motion while the symmetric top falls from  $\theta = 0$  to  $\theta = \theta_{max}$ .

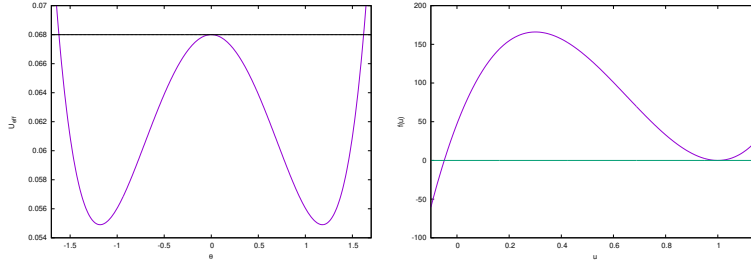


Figure 35:  $U_{eff}$ ,  $E'$  (straight black line),  $Mglb/a$  (dotted line) at left, and  $f(u)$  at right.  $E'$  and  $Mglb/a$  are overlapped since they are equal. This case gives spiral like motion, and initial values for this case as follows;  $\theta_0 = 1.619rad$ ,  $\dot{\theta}_0 = 0$ ,  $\dot{\psi}_0 = 20.90rad/s$ ,  $\dot{\phi}_0 = 31.95rad/s$  and resulting  $E' = 0.06800J$ . Turning angles for  $\theta$  are  $-1.619$  and  $1.619rad$ , and the minimum of  $U_{eff}$  is at  $1.182rad$ .  $f(u)$  has roots at  $u = -0.04866$  and  $u = 1$ , corresponding to  $\theta = 1.619$  and  $\theta = 0$ . For this case constants of the motion are  $b = a = 30.4$  and  $\alpha = \beta = 971.4$ .

We see the results obtained by using Eq. (33) in Fig. 36 for initial values  $\theta_0 = 1.619rad$ ,  $\dot{\theta}_0 = 0$ ,  $\dot{\phi}_0 = 31.95rad/s$  and  $\dot{\psi}_0 = 20.90rad/s$ . With these

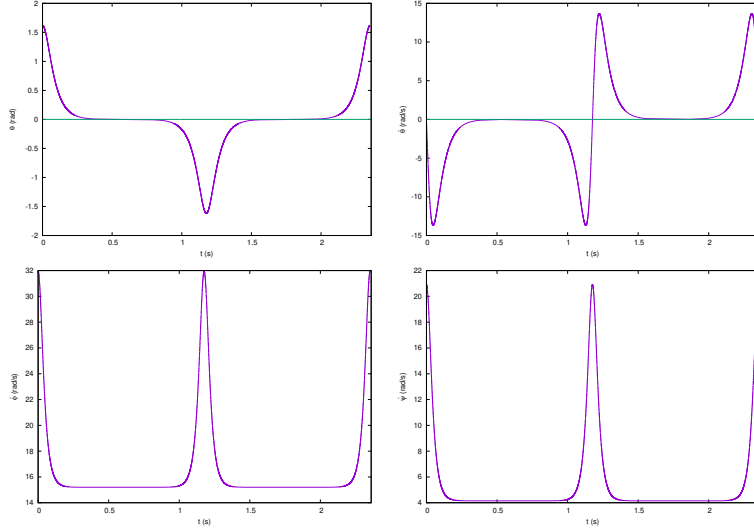


Figure 36:  $\theta$ (up left),  $\dot{\theta}$ (up right),  $\dot{\phi}$ (down left) and  $\dot{\psi}$ (down right) are obtained from the integration of Eq. (33). Initial values are the same as Fig. 35.

initial values  $b = a = 30.40$  and  $\alpha = \beta = 971.4$ . From the figure, we can say that  $\theta$  starts with the maximum value and decreases negative of that maximum value and the symmetric top passes from  $\theta = 0$  point.

It is seen from Fig. 35 that when  $\theta$  is close to zero,  $\dot{\theta}$  will be close to zero. So the symmetric top spends more time at these  $\theta$  values. Results of this are seen in Fig. 36;  $\dot{\theta}$ ,  $\dot{\phi}$  and  $\dot{\psi}$  do not change much when  $\theta$  is close to zero. If we look at  $\dot{\phi}$  as the symmetric top rises ( $\theta$  decreases), it decreases. But, this decrease is not enough for fall of the symmetric top; it rises till  $\theta$  reaching 0 and falls from a different side. If we consider  $b = \dot{\phi} \sin^2 \theta + a \cos \theta$ ; as  $\theta$  decreases the contribution from  $a$  increases and to obey conservation of the angular momentum in  $z'$ -direction  $\dot{\phi}$  should also decrease. If we consider  $a = (I_z/I_x)(\dot{\psi} + \dot{\phi} \cos \theta)$ ; the contribution from  $\dot{\phi}$  increases since  $\cos \theta$  increases faster, then  $\dot{\psi}$  should also decrease to obey conservation of the angular momentum in  $z$ -direction. The following part of the motion is something like an inverted structure of this as  $\theta$  goes to  $-\theta_{max}$ . After  $\theta$  reaching  $-\theta_{max}$ , the above procedure will take place in the reverse order.

In Fig. 37, we see results obtained from the numerical integration of

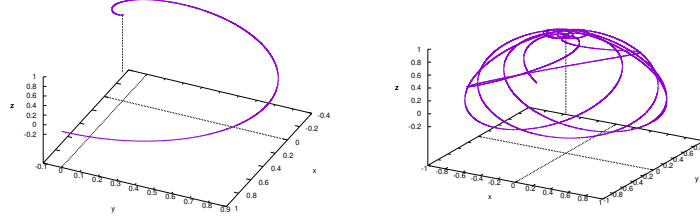


Figure 37: Shapes of the locus on unit sphere for spiraling motion. Initial values are the same as Fig. 35. ( Animated version is available at <https://youtu.be/TjYqZDDUZMY> .)

Eq.s (36). It is seen that from  $\theta = \theta_{max}$  to 0 the symmetric top makes a spiraling motion. The other results obtained from the integration of angular accelerations can be found in the appendix, Fig. 53.

If we consider torque and angular momentum, at the beginning  $\dot{\phi}$  causes an inertial torque greater than the gravitational one and top rises. This inertial torque is enough to rise the symmetric top to  $\theta = 0$  point and then top falls from a different side by the effect of gravitational torque. This fall causes an increase in  $\dot{\phi}$  and at  $\theta = \theta_{max}$  the symmetric top starts to rise again. This motion repeats itself.

Here, it will be better to consider this case with dissipation. If we put a spinning gyroscope or symmetric top in the sleeping top position,  $\theta = 0$ , its spin will decrease as time passes due to dissipation. If at the beginning  $|a| > \sqrt{4Mgl/I_x}$ , small deviations from the sleeping top will result in a return of the symmetric top to the sleeping position. As time passes the spin of the symmetric top will slow down and  $|a|$  will be smaller than  $\sqrt{4Mgl/I_x}$ . In this case, the motion will look like  $b = a$  and  $E' = Mglb/a$  case, and the symmetric top will fall slowly with a spiraling motion. This motion can be seen from gyroscopes. However, the situation for child's top is a bit different. As child's top falls the contact point with the surface changes, when this combines with impurities we see wobbling motion.

### 3.13 Motion over the bump

The last case, that we will consider here is  $b = a$ ,  $E' > Mglb/a$  and  $|a| < \sqrt{4Mgl/I_x}$ . In this case, the motion will look like the motion through pseudo-

regular points, but in this case, we have a bump. In Fig. 38, we see  $U_{eff}$  together with  $E'$  and  $f(u)$  for such a case. From the effective potential graph, if the symmetric top starts its motion from  $\theta_{max}$  we can say that  $\dot{\theta}$  will have negative values at the beginning to rise the symmetric top. The magnitude of  $\dot{\theta}$  will reach its maximum when  $U_{eff}$  is at the minimum. Then we will see the effect of the bump; the magnitude of  $\dot{\theta}$  will decrease till  $\theta$  reaching to 0. At  $\theta = 0$ , the symmetric top will fall to the other side with its negative  $\dot{\theta}$  value till  $\theta$  reaching  $-\theta_{max}$ . Then the motion will take place in the reverse order.

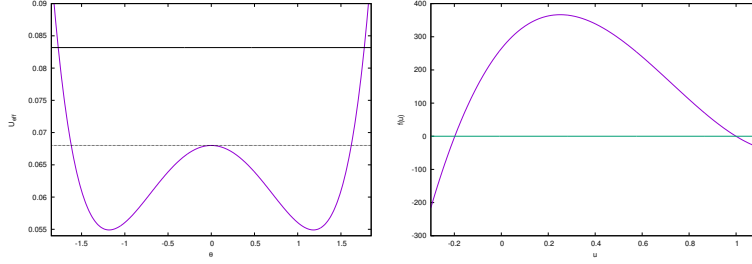


Figure 38:  $U_{eff}$ ,  $E'$  (straight black line),  $Mglb/a$  (dotted line) at left, and  $f(u)$  at right. This case gives a motion over a bump, and initial values for this case as follows;  $\theta_0 = 1.770rad$ ,  $\dot{\theta}_0 = 0$ ,  $\dot{\psi}_0 = 26.85rad/s$ ,  $\dot{\phi} = 37.91rad/s$  and resulting  $E' = 0.08318$ . Turning angles for  $\theta$  are  $-1.770$  and  $1.770rad$ , and the minimum of  $U_{eff}$  is at  $1.182rad$ . The roots of  $f(u)$  occurs at  $u = -0.1981$  and  $u = 1$  corresponding to  $\theta = 1.770rad$  and  $\theta = 0$ . Constants of motion:  $b = a = 30.40$  and  $\alpha = 1188$ .

In Fig. 39, we see the results obtained by using Eq. (33) for initial values  $\theta_0 = 1.770rad$ ,  $\dot{\theta}_0 = 0$ ,  $\dot{\psi}_0 = 26.85rad/s$  and  $\dot{\phi} = 37.91rad/s$ . We see that the change in  $\dot{\theta}$  at the local maximum of the effective potential does not affect too much  $\dot{\phi}$  and  $\dot{\psi}$ . Change in  $\dot{\phi}$  and  $\dot{\psi}$  is similar to the motion through pseudo-singular points case. Explanations will be similar to that case.

In Fig. 40, we see results obtained by numerical integration of angular accelerations. The symmetric top goes to  $\theta = 0$  point after making a curve and then falls from a different side, this repeats itself and at each case it passes from  $\theta = 0$  point with different crossings. The other results are available in the appendix, Fig. 54.

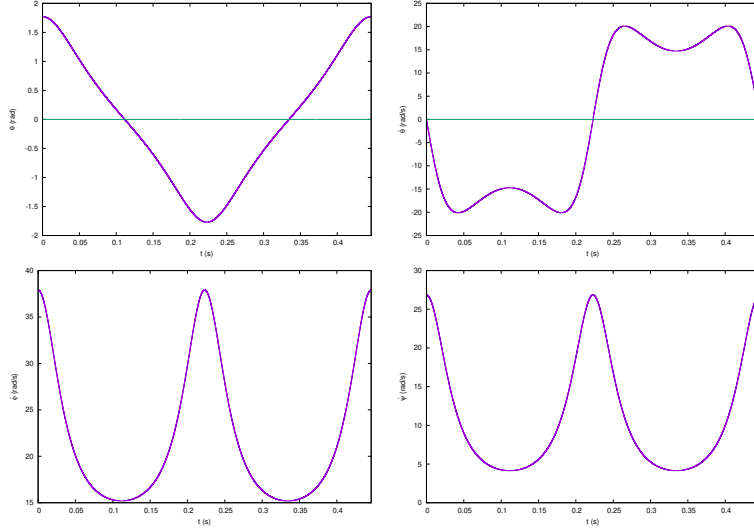


Figure 39:  $\theta$ (up left),  $\dot{\theta}$ (up right),  $\dot{\phi}$ (down left) and  $\dot{\psi}$ (down right) are obtained from the integration of Eq. (33). Initial values are the same as Fig. 32.

## 4 Summary

We have studied the symmetric top problem in detail. This study showed that there are some previously unnoticed interesting situation related to the motion of the symmetric top. We also have learned that the inertial torque arising from the non-inertial structure of the spinning symmetric top rises it. This inertial torque shows itself in the effective potential via constants  $a$  and  $b$ , which correspond conserved angular momenta in  $z$  and  $z'$ -direction respectively. After writing the effective potential we see that  $\theta$  changes mostly between two turning angles in accordance with conservation of energy.

The inertial torque originated from  $\vec{\omega} \times \vec{L}$  term in Euler equations is responsible from both precession and nutation. A component of it in  $z'$ -direction causes precession, and another component in the direction of the line of nodes causes nutation. These components can change throughout the motion, depending on the content of the  $\vec{\omega} \times \vec{L}$ . In the precession,  $\dot{\theta}$  plays a role by causing change in  $\dot{\phi}$ , and in the nutation  $\dot{\phi}$  plays a role with contributing inertial torque.

We also have seen that conservation of angular momenta is vital for un-

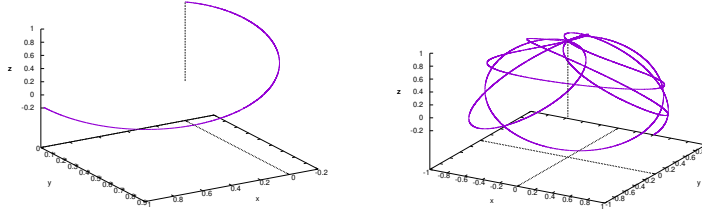


Figure 40: Shapes of the locus on unit sphere for motion over the bump. Initial values are the same as Fig. 38. ( Animated version is available at <https://youtu.be/DCNZ66Y1GnE> .)

derstanding the motion of the symmetric top. It can keep the symmetric top from  $\theta = 0$  point, or force it to pass from that point depending on values of angular momenta. We have seen that conservation of angular momentum can change spin direction of the symmetric top in an unimaginable way.

## References

- [1] Routh, E. J., "Advanced Dynamics of a System of Rigid Bodies", 6th Ed., Dover, 1955.
- [2] Klein, F. and Sommerfeld, A., "The theory of the Top, Volume II", Birkhauser, 2010.
- [3] Gregory, R. D., "Classical Mechanics", Cambridge University Press, 2006.
- [4] MacMillan, W. D., "Dynamics Of Rigid Bodies", Dover, 1960.
- [5] Groesberg, S. W., "Advanced mechanics", Wiley, 1968.
- [6] Goldstein, H., "Classical Mechanics", 2nd Ed., Addison-Wesley, 1980.
- [7] Landau, L. D. and Lifshitz, E. M., "Mechanics", 3rd Ed., Butterworth-Heinenann, 2000.
- [8] Symon, K.R., "Mechanics", 3rd Ed., Addison-Wesley, 1971.



[9] Greiner, W., "Classical Mechanics", Springer, 2003.

[10] Hauser, W. "Introduction to the principles of mechanics", Addison-Wesley, 1965.

## 5 Appendix

Graphs for  $\theta$ ,  $\phi$ ,  $\psi$ ,  $\dot{\theta}$ ,  $\dot{\phi}$  and  $\dot{\psi}$  for the above cases, these are obtained from the numerical solutions of the angular accelerations.

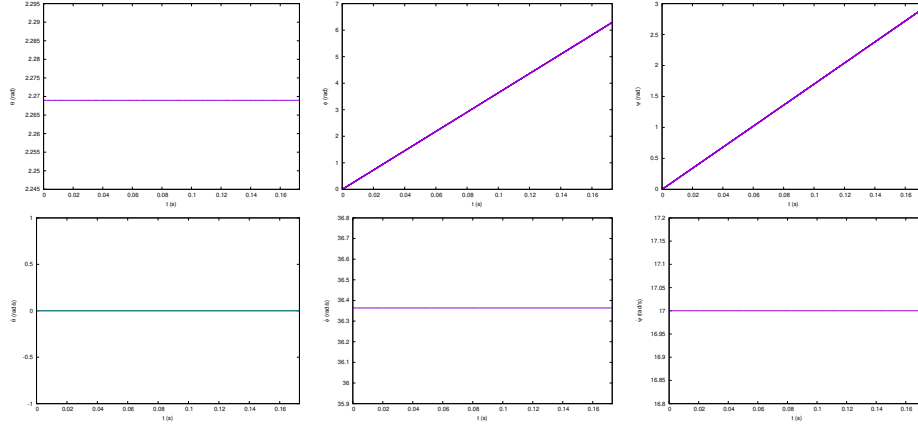


Figure 41: Regular precession with single  $\dot{\phi}$ ;  $\theta$  (up left),  $\phi$  (up middle),  $\psi$  (up right),  $\dot{\theta}$  (down left),  $\dot{\phi}$  (down middle) and  $\dot{\psi}$  (down right) for initial values  $\theta_0 = 2.269\text{rad}$ ,  $\phi_0 = 0$ ,  $\psi_0 = 0$ ,  $\dot{\theta}_0 = 0$ ,  $\dot{\phi}_0 = 36.36\text{rad/s}$  and  $\dot{\psi}_0 = 17\text{rad/s}$ .

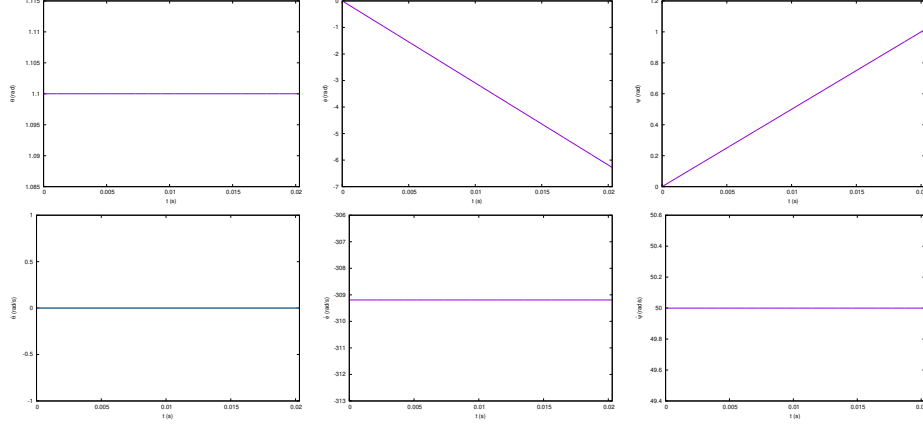


Figure 42: Regular precession with two  $\dot{\phi}$ ;  $\theta$  (up left),  $\phi$  (up middle),  $\psi$  (up right),  $\dot{\theta}$  (down left),  $\dot{\phi}$  (down middle) and  $\dot{\psi}$  (down right) for initial values  $\theta_0 = 1.1\text{rad}$ ,  $\phi_0 = 0$ ,  $\psi_0 = 0$ ,  $\dot{\theta}_0 = 0$ ,  $\dot{\phi}_0 = -309.2\text{rad/s}$  and  $\dot{\psi}_0 = 50\text{rad/s}$ .

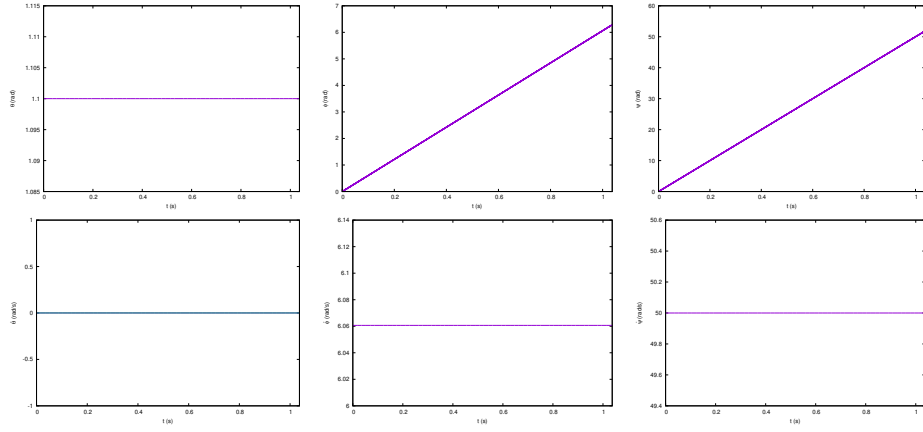


Figure 43: Regular precession with two  $\dot{\phi}$ ;  $\theta$  (up left),  $\phi$  (up middle),  $\psi$  (up right),  $\dot{\theta}$  (down left),  $\dot{\phi}$  (down middle) and  $\dot{\psi}$  (down right) for initial values  $\theta_0 = 1.1\text{rad}$ ,  $\phi_0 = 0$ ,  $\psi_0 = 0$ ,  $\dot{\theta}_0 = 0$ ,  $\dot{\phi}_0 = 6.061\text{rad/s}$  and  $\dot{\psi}_0 = 50\text{rad/s}$ .

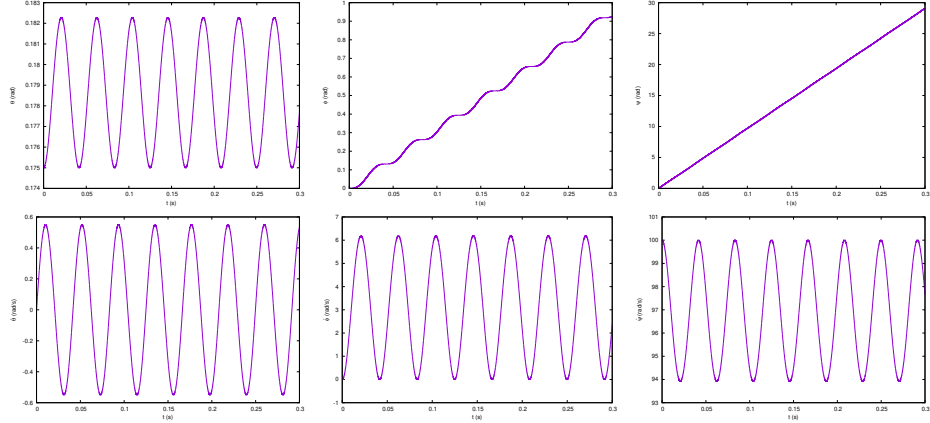


Figure 44: Cup like motion, changes in  $\theta$  (up left),  $\phi$  (up middle),  $\psi$  (up right),  $\dot{\theta}$  (down left),  $\dot{\phi}$  (down middle) and  $\dot{\psi}$  (down right) as time changes for initial values  $\theta_0 = 0.175\text{rad}$ ,  $\phi_0 = 0$ ,  $\psi_0 = 0$ ,  $\dot{\theta}_0 = 0$ ,  $\dot{\phi}_0 = 0$  and  $\dot{\psi}_0 = 100\text{rad/s}$ .

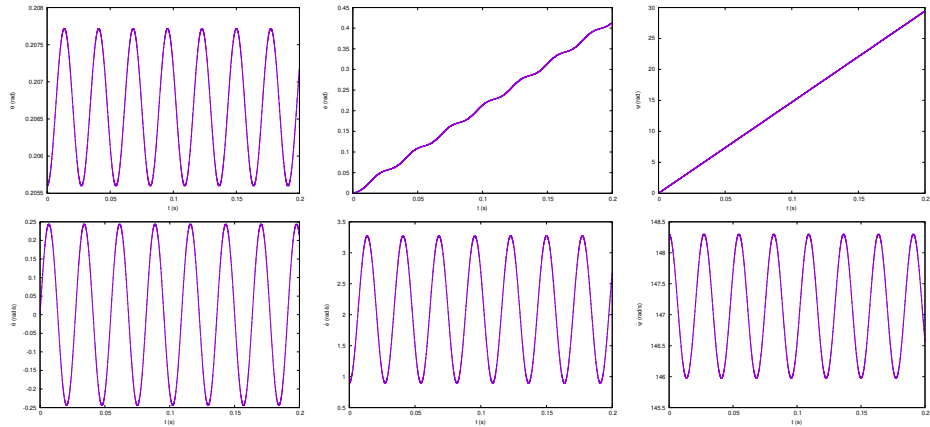


Figure 45: Wavy precession, changes in  $\theta$  (up left),  $\phi$  (up middle),  $\psi$  (up right),  $\dot{\theta}$  (down left),  $\dot{\phi}$  (down middle) and  $\dot{\psi}$  (down right) as time changes for initial values  $\theta_0 = 0.2056\text{rad}$ ,  $\phi_0 = 0$ ,  $\psi_0 = 0$ ,  $\dot{\theta}_0 = 0$ ,  $\dot{\phi}_0 = 0.8968\text{rad/s}$  and  $\dot{\psi}_0 = 148.3\text{rad/s}$ .

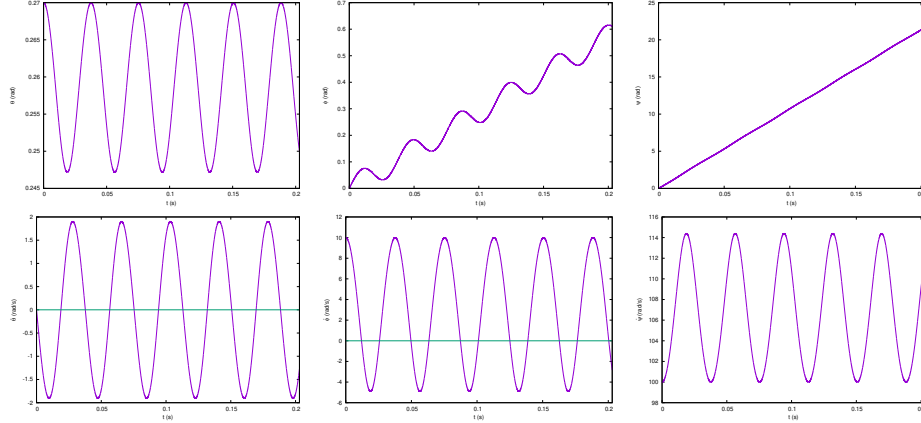


Figure 46: Looping motion, changes in  $\theta$  (up left),  $\phi$  (up middle),  $\psi$  (up right),  $\dot{\theta}$  (down left),  $\dot{\phi}$  (down middle) and  $\dot{\psi}$  (down right) as time changes for initial values  $\theta_0 = 0.270\text{rad}$ ,  $\phi_0 = 0$ ,  $\psi_0 = 0$ ,  $\dot{\theta}_0 = 0\text{rad/s}$ ,  $\dot{\phi}_0 = 10\text{rad/s}$  and  $\dot{\psi}_0 = 100\text{rad/s}$ .

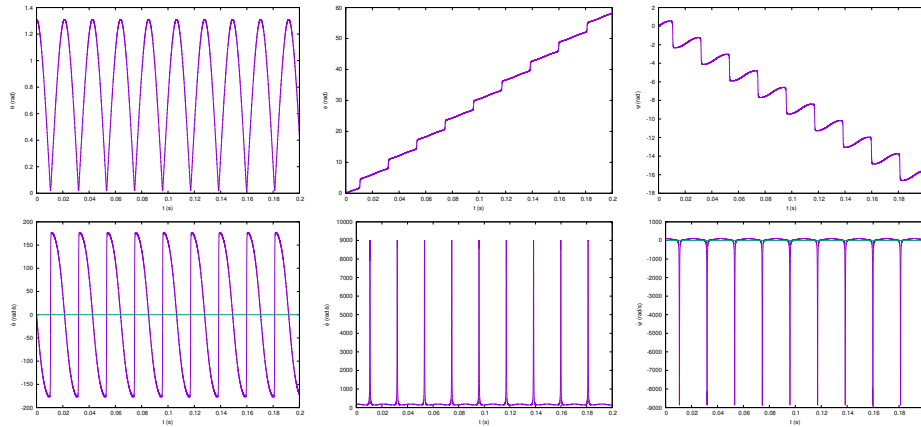


Figure 47: Precession with single nutation, changes in  $\theta$  (up left),  $\phi$  (up middle),  $\psi$  (up right),  $\dot{\theta}$  (down left),  $\dot{\phi}$  (down middle) and  $\dot{\psi}$  (down right) as time changes for initial values  $\theta_0 = 1.310\text{rad}$ ,  $\phi_0 = 0$ ,  $\psi_0 = 0$ ,  $\dot{\theta}_0 = 0\text{rad/s}$ ,  $\dot{\phi}_0 = 190\text{rad/s}$  and  $\dot{\psi}_0 = 100\text{rad/s}$ .

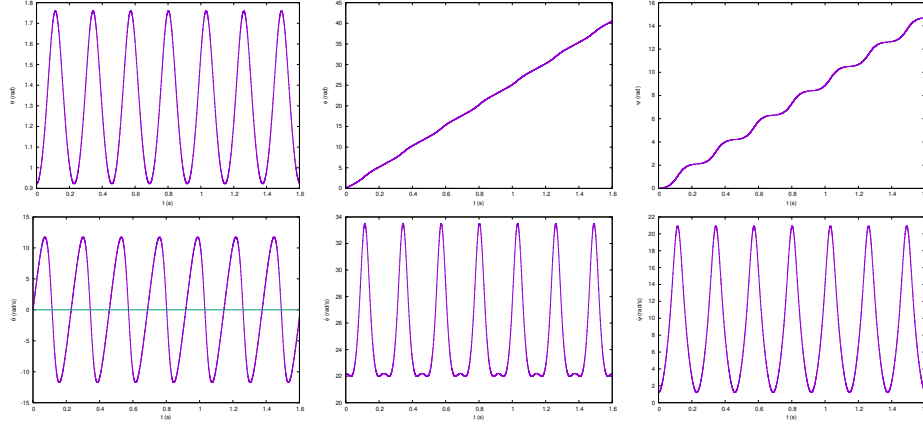


Figure 48: Precession with single nutation for weak top, changes in  $\theta$  (up left),  $\phi$  (up middle),  $\psi$  (up right),  $\dot{\theta}$  (down left),  $\dot{\phi}$  (down middle) and  $\dot{\psi}$  (down right) as time changes for initial values  $\theta_0 = 0.9225\text{rad}$ ,  $\phi_0 = 0$ ,  $\psi_0 = 0$ ,  $\dot{\theta}_0 = 0\text{rad/s}$ ,  $\dot{\phi}_0 = 22.21\text{rad/s}$  and  $\dot{\psi}_0 = 1.225\text{rad/s}$ .

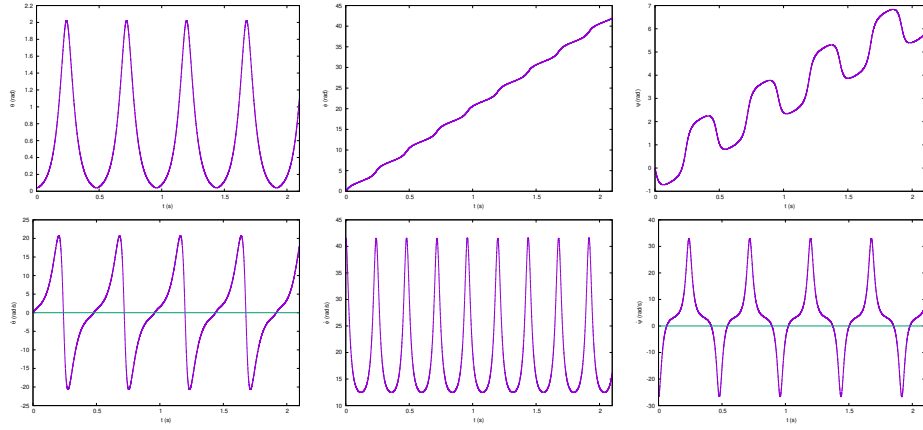


Figure 49: Motion with same precessional angular velocity at extrema, changes in  $\theta$  (up left),  $\phi$  (up middle),  $\psi$  (up right),  $\dot{\theta}$  (down left),  $\dot{\phi}$  (down middle) and  $\dot{\psi}$  (down right) as time changes for initial values  $\theta_0 = 0.04097\text{rad}$ ,  $\phi_0 = 0$ ,  $\psi_0 = 0$ ,  $\dot{\theta}_0 = 0\text{rad/s}$ ,  $\dot{\phi}_0 = 41.51\text{rad/s}$  and  $\dot{\psi}_0 = -26.59\text{rad/s}$ .

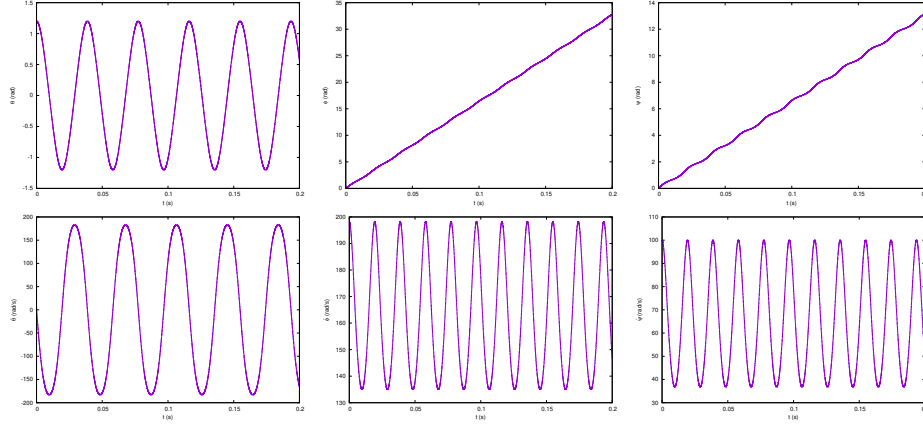


Figure 50: Motion through pseudo-singular points, changes in  $\theta$  (up left),  $\phi$  (up middle),  $\psi$  (up right),  $\dot{\theta}$  (down left),  $\dot{\phi}$  (down middle) and  $\dot{\psi}$  (down right) as time changes for initial values  $\theta_0 = 1.200\text{rad}$ ,  $\phi_0 = 0$ ,  $\psi_0 = 0$ ,  $\dot{\theta}_0 = 0$ ,  $\dot{\phi}_0 = 198.2\text{rad/s}$  and  $\dot{\psi}_0 = 100\text{rad/s}$ .

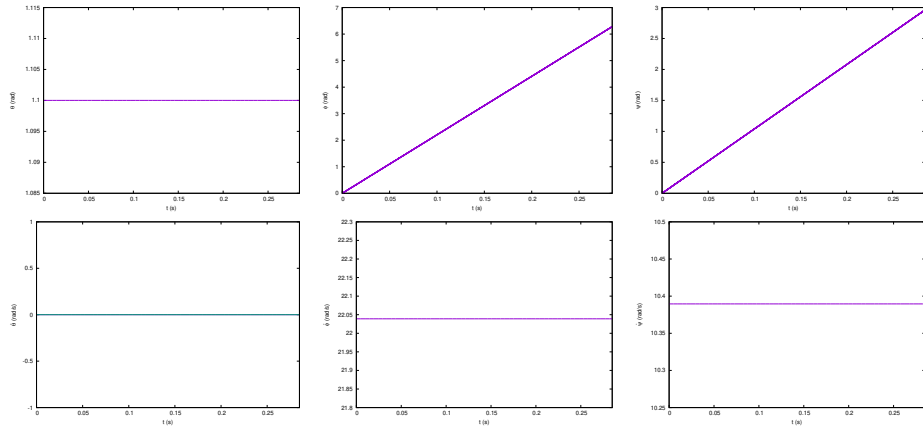


Figure 51: Regular precession when  $b = a$ , changes in  $\theta$  (up left),  $\phi$  (up middle),  $\psi$  (up right),  $\dot{\theta}$  (down left),  $\dot{\phi}$  (down middle) and  $\dot{\psi}$  (down right) as time changes for initial values  $\theta_0 = 1.1\text{rad}$ ,  $\phi_0 = 0$ ,  $\psi_0 = 0$ ,  $\dot{\theta}_0 = 0$ ,  $\dot{\phi}_0 = 22.04\text{rad/s}$  and  $\dot{\psi}_0 = 10.39\text{rad/s}$ .

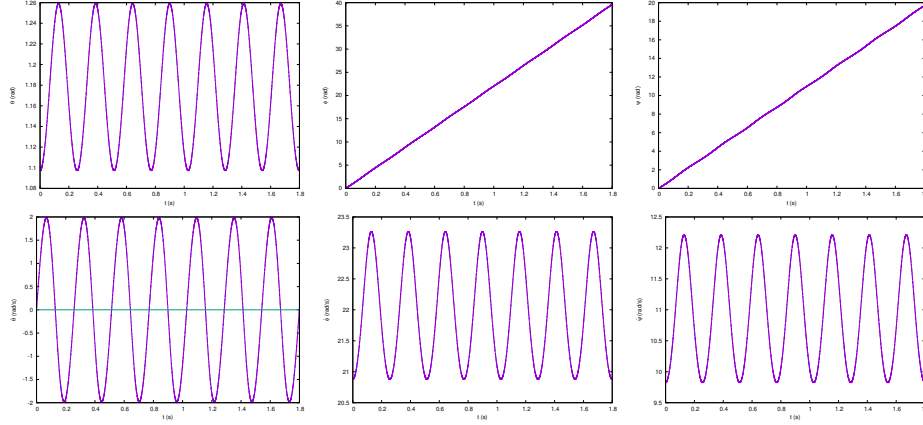


Figure 52: Precession in one direction when  $b = a$ , changes in  $\theta$  (up left),  $\phi$  (up middle),  $\psi$  (up right),  $\dot{\theta}$  (down left),  $\dot{\phi}$  (down middle) and  $\dot{\psi}$  (down right) as time changes for initial values  $\theta_0 = 1.097rad$ ,  $\phi_0 = 0$ ,  $\psi_0 = 0$ ,  $\dot{\theta}_0 = 0rad/s$ ,  $\dot{\phi}_0 = 20.88rad/s$  and  $\dot{\psi}_0 = 9.824rad/s$ .

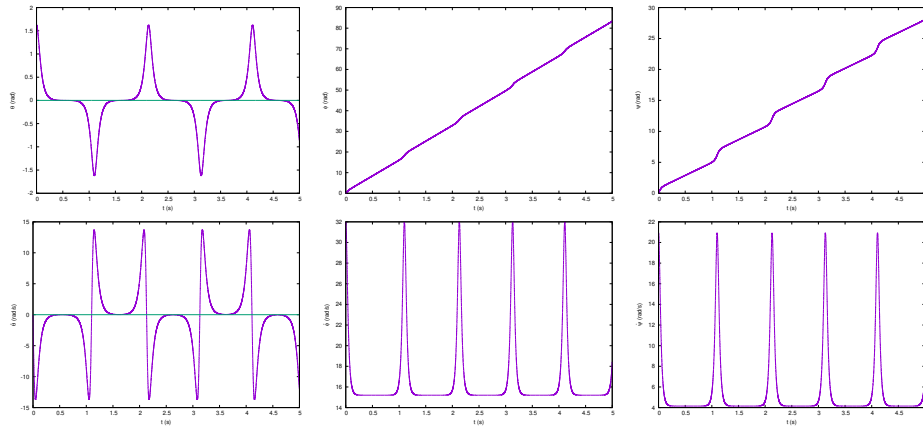


Figure 53: Spiralling motion, changes in  $\theta$  (up left),  $\phi$  (up middle),  $\psi$  (up right),  $\dot{\theta}$  (down left),  $\dot{\phi}$  (down middle) and  $\dot{\psi}$  (down right) as time changes for initial values  $\theta_0 = 1.619rad$ ,  $\phi_0 = 0$ ,  $\psi_0 = 0$ ,  $\dot{\theta}_0 = 0$ ,  $\dot{\phi}_0 = 31.95rad/s$  and  $\dot{\psi}_0 = 20.90rad/s$ .

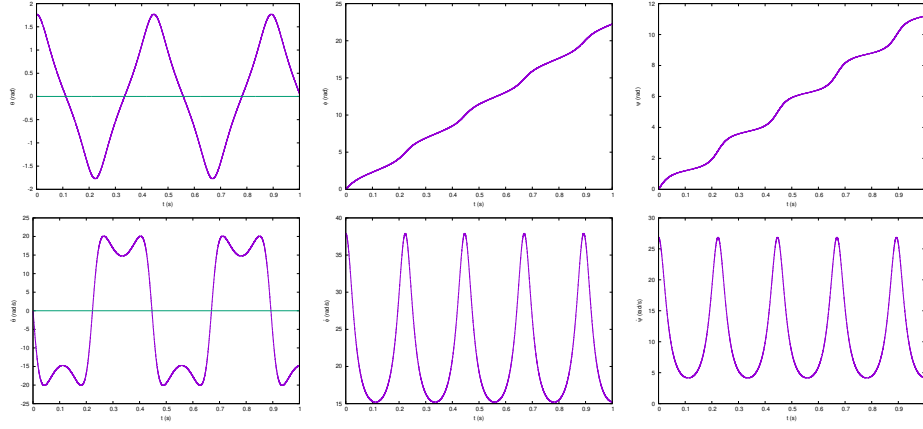


Figure 54: Motion over the bump, changes in  $\theta$  (up left),  $\phi$  (up middle),  $\psi$  (up right),  $\dot{\theta}$  (down left),  $\dot{\phi}$  (down middle) and  $\dot{\psi}$  (down right) as time changes for initial values  $\theta_0 = 1.770rad$ ,  $\phi_0 = 0$ ,  $\psi_0 = 0$ ,  $\dot{\theta}_0 = 0$ ,  $\dot{\phi}_0 = 37.91rad/s$  and  $\dot{\psi}_0 = 26.85rad/s$ .